Removal of Trace Heavy Metals from Drinking Water by Electrocoagulation

Joe Heffron
Marquette University

Removal of Trace Heavy Metals from Drinking Water by Electrocoagulation

Joe Heffron

A thesis submitted to the faculty of the Graduate School,
Marquette University, in partial fulfillment of the requirements for the degree of
Master of Science in Civil Engineering
Milwaukee, Wisconsin
April 2015

ABSTRACT

Removal of Trace Heavy Metals from Drinking Water by Electrocoagulation

Joe Heffron

Marquette University, 2015

Geologic and anthropogenic heavy metals contaminate drinking water for hundreds of millions of people worldwide. Electrocoagulation – the *in situ* generation of coagulant by electrolytic oxidation of metal electrodes – is a century-old process gaining new traction for metal removal from water and wastewater. However, the low conductivity of drinking water and low target contaminant concentrations required for human consumption present challenges for electrocoagulation of drinking water. This study is unique in that it addresses seven different metal contaminants at the trace concentrations of concern to human consumption and investigates the wide range of possible source water matrices.

The goal of this study was to determine the feasibility of electrocoagulation to remove trace heavy metals from drinking water. This goal was addressed by first demonstrating removal of contaminant metals to below regulatory concentrations. Seven metals were tested for removal to meet U.S. Environmental Protection Agency requirements for drinking water: chromium, nickel, copper, zinc, arsenic, cadmium and lead. Next, the effects of electrode material (aluminum versus iron) and post-treatment separation of flocs (micro-filtration versus settling alone) were tested in a mixed-contaminant scenario. In addition, the importance of source water pH and ionic composition was tested for the same five metals. A bench-scale, batch reactor was used with a galvanostatic DC power supply providing 0.5 A current. Metal concentrations were determined by inductively-coupled plasma mass spectrometry (ICP-MS).

Removal of five metals was demonstrated to below regulatory concentrations for drinking water: chromium, copper, arsenic, cadmium and lead. Iron electrodes vastly out-performed aluminum electrodes in removing chromium and arsenic. Aluminum electrodes were slightly more effective at removing nickel, cadmium and lead, but only at pH 6.5. Microfiltration enhanced contaminant removal and reduced the variance of effluent concentration. Microfiltration also dramatically reduced the residual concentration of aluminum and iron after treatment. Electrocoagulation removed nickel and cadmium more efficiently at pH 8.5 than 6.5, though chromium, arsenic and lead showed no significant effect from initial pH in the range tested. All metals exhibited poorer removal efficiencies as the ionic strength of the background electrolyte increased, particularly in the very high-solids, synthetic groundwaters.

ACKNOWLEDGEMENTS

Funding for this project was provided by the Industry University Collaborative Research Program for Water Equipment & Policy in Milwaukee, Wisconsin, USA, under NSF Grant Number 0968844. This project would not have been possible without the help of Mike Dollhopf, laboratory manager for the Water Quality Center at Marquette University. Mr. Dollhopf performed all ICP-MS analyses. In addition, invaluable guidance for this project was provided by Ms. Chen Li, Water Treatment Engineer at A.O. Smith Corporation. Many of the tests that comprise this thesis were performed by Matt Marhefke, an undergraduate researcher in the Water Quality Center in the summer of 2014. Mr. Marhefke was often the spirit that kept the team pressing forward in the lab. Many thanks are due to my fellow researchers in the Water Quality Center, especially to the Mayer lab group. Thanks also go to Dr. Naveen Bansal of the Department of Mathematics, Statistics and Computer Science at Marquette for offering advice on the statistical methods used in this study. Finally, I owe immense gratitude to my advisor and P.I., Dr. Brooke Mayer, P.E., who took me on for this project and offered me the tremendous opportunity to work and study at Marquette.

DEDICATION

This thesis is dedicated to my wife, Sierra, who moved far from her family to the frigid North, forever chasing this crazy dream of electrocoagulation.

TABLE OF CONTENTS

LIST OF TABLES

LIST OF FIGURES

1. INTRODUCTION

1.1. Electrocoagulation

Electrocoagulation (EC) is the *in situ* production of coagulant in water by passing electrical charge through one or more submerged, sacrificial electrodes. EC can be modeled as a three-stage process: coagulant formation, contaminant destabilization and flocculation (Fernandes et al., 2014; Liu et al., 2010). First, the anode is electrochemically oxidized to release cations in solution:

$$\mathrm{M}^{0}_{(s)} \longrightarrow \mathrm{M}^{z+}_{(aq)} + z \cdot e^{-} \qquad \text{(Rxn 1.1)}$$

where M is the metal comprising the sacrificial electrode(s), commonly aluminum or iron. These cations combine with hydroxide ligands to form coagulant in solution. At the same time, hydrogen gas is formed at the cathode by electrolytic reduction of water. Next, the coagulant destabilizes dissolved or colloidal contaminants and physically aggregates to form flocs. Flocs may enmesh bubbles of hydrogen gas and rise to the surface to form a flotation layer or simply settle by gravitation. These three processes are depicted in Figure 1.1.

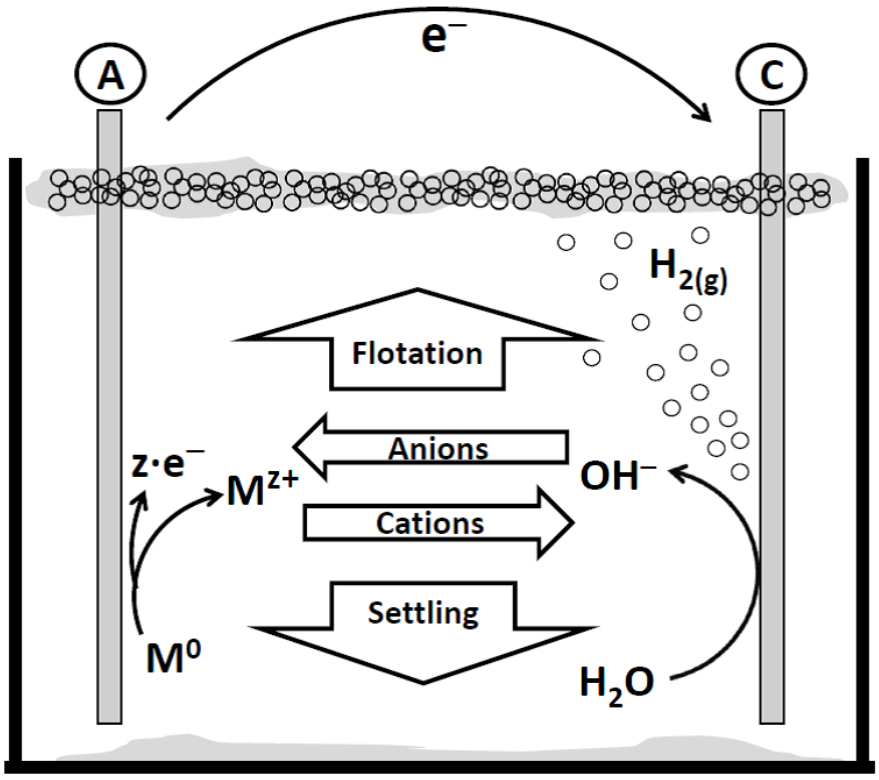

Figure 1.1: Summary of primary reactions and transport in an electrocoagulation reactor. Flocs formed by coagulation are separated by gravity either by sedimentation or flotation. Charged species in solution undergo electrophoretic movement, with negative charge flowing toward the anode and positive charge toward the cathode.

1.2. History

EC was first patented in the late 19th century as a sewage treatment process. The first operational EC wastewater treatment facilities appeared in the 1890s in London and Salford, England. These early plants combined the wastewater influent with seawater to increase conductivity and generate chlorine disinfectant. In both Oklahoma City, OK, and Santa Monica, CA, EC wastewater facilities began operation in 1911. EC was also proposed for potable water treatment. In 1925, a power plant near Moscow began treating drinking water with EC using soluble iron electrodes. In the 1940s and '50s, EC pilot plants using iron and aluminum electrodes were tested for color and turbidity removal from drinking water (Vik et al., 1984).

Though the EC facilities touted high quality effluent, operational costs were considered high at the time due to the need to haul sludge from the treatment plants (Vik et al., 1984). Furthermore, federal regulations did not provide minimum standards for secondary treatment of wastewater until 1972 (Metcalf and Eddy et al., 2003), which offered little incentive to continue providing premium treatment. In addition, chemical coagulants for water treatment were becoming less expensive (Holt et al., 2005). EC did not gain wide adoption for drinking water treatment, and all EC wastewater facilities in the U.S. were decommissioned by 1930 (Holt et al., 2005).

With contemporary regulations and methods for detecting contaminants, interest in EC has seen a recent resurgence as an effective and portable option for water and wastewater treatment. Recent applications include remediation of wastewaters from pulp mills (Perng et al., 2009), acid mine drainage (Radić et al., 2014), textile manufacturers (Bhatnagar et al., 2014), restaurants (Chen et al., 2000), slaughterhouses (Ozyonar & Karagozoglu, 2014), and pharmaceutical manufacturers (Farhadi et al., 2012). EC effectively removes a wide range of pollutants, including metals (Li et al., 2012), natural organic matter (NOM) (Dubrawski & Mohseni, 2013b), algae (Gao et al., 2010), viruses (Tanneru et al., 2013), and oil and grease (Chen et al., 2000).

To date, most research into EC has focused on wastewater applications rather

than drinking water. Wastewater conductivity is higher than that of drinking water and can be increased by adding salts. Relatively few companies have produced commercial EC reactors. In the U.S., EC wastewater treatment units are produced by Powell Water Systems, Inc. (2002), Quantum Ionics, Inc. (2004), and Water Tectonics (2015). Jye-Shi, Inc., of Taiwan also produces an EC unit for industrial wastewater treatment (Perng et al., 2009). Lamar University in Texas has created a pilot-scale, mobile treatment unit for arsenic removal from drinking water. The mobile plant uses a series of iron electrodes and features air sparging to enhance oxidation (Parga et al., 2012).

1.3. Comparison to conventional coagulation

EC has numerous benefits over conventional coagulation with metal salts. The EC process is easy and safe to operate, can be automated, requires shorter residence times, and produces smaller volumes of sludge (Cataldo Hernández et al., 2012; Mouedhen et al., 2008; Ozyonar & Karagozoglu, 2014; Zhu et al., 2005). Unlike conventional coagulation, EC can be effective over a wide initial pH range, because hydrolysis at the cathode neutralizes the solution pH over time (Bagga et al., 2008; Mouedhen et al., 2008; Zhu et al., 2005). EC's portability has led some authors to suggest remote and emergency applications as an appropriate niche (Bagga et al., 2008; Holt et al., 2005).

The electrical potential across the EC cell provides several additional advantages over chemical coagulation. EC offers better removal efficiency for many contaminants than conventional coagulation and removes smaller diameter colloids due to electrophoretic transport and concentration of charged particles (Behloul et al., 2013; de Mello Ferreira et al., 2013; Ozyonar & Karagozoglu, 2014). With the benefit of flotation due to hydrolysis, EC could theoretically replace both chemical coagulation and dissolved air flotation (DAF) processes (Vik et al., 1984). Moreover, EC can oxidize or reduce contaminants like arsenic and chromium that would require pre-treatment when using conventional coagulation (Ratna Kumar et al., 2004). Given the appropriate application, EC could therefore replace chemical coagulation, DAF and chemical pre-treatment.

In potable water applications, EC has the benefit of not adding additional anions

(*e.g.*, chloride or sulfate) into solution. However, the very low conductivity of most potable water means that the applied voltage (and therefore power) required is much greater than for wastewater applications (Dubrawski & Mohseni, 2013a; de Mello Ferreira et al., 2013). The primary drawback of EC, therefore, is that electrical energy is required for operation, as opposed to the convenient chemical energy embodied in aluminum or iron salts. The electrical energy demand for treatment increases as conductivity decreases. For drinking water applications, the low conductivity of the electrolyte requires closely-spaced electrodes with broad surface areas. An electrode with a large surface area has a lower current density, and therefore produces fewer hydrogen bubbles per unit area. Therefore, drinking water applications may not be able to rely on flotation for floc removal (Dubrawski & Mohseni, 2013a).

1.4. Mechanisms

1.4.1 Electrolytic dissolution

The first step in the *in situ* formation of coagulant is the oxidation/dissolution of the sacrificial anode. Ideal anodic dissolution from charge transfer is given by Faraday's Law of Electrolysis:

$$m = \frac{I \cdot t \cdot M}{z \cdot F} \tag{1.1}$$

where m is the mass liberated from the anode (g), I is the current (A), t is reaction time (s), M is molar mass (g/mol), z is valence number and F is Faraday's constant (C/mol) (Abdel-gawad et al., 2012; Akbal & Camcı, 2012; Dubrawski & Mohseni, 2013a; de Mello Ferreira et al., 2013). The Faraday efficiency (Φ) of the reactor is thus the actual mass (m_{actual}) of ions released compared to the theoretical mass ($m_{theoretical}$) given by Faraday's Law.

$$\Phi = \frac{m_{actual}}{m_{theoretical}} \tag{1.2}$$

The actual rate of coagulant production can exceed the theoretical mass transfer given by Faraday's Law and depends on not only current but also the pH and composition of the electrolyte (Cataldo Hernández et al., 2012; Chen et al., 2000; Mouedhen et al., 2008; Vepsäläinen et al., 2012). Chemical oxidation of the cathode in solution may contribute significantly to the total coagulant in the system. Moreover, acidic and alkaline microenvironments form around the anode and cathode, respectively, and promote chemical attack on the electrodes. Aluminum in particular is amphoteric and corrodes below pH 4 and above pH 8.5 (Mouedhen et al., 2008).

As metal ions are released at the anode, hydroxide ions and hydrogen gas are created through hydrolysis at the cathode (Akbal & Camcı, 2012; Bhatnagar et al., 2014; de Mello Ferreira et al., 2013; Dubrawski & Mohseni, 2013a; Fernandes et al., 2014; Holt et al., 2005; van Genuchten et al., 2014).

$$2\,H_2O + 2\,e^- \longrightarrow H_{2(g)} + 2\,OH^- \qquad \text{(Rxn 1.2)}$$

The evolution of hydroxide ions at the cathode serves to increase bulk pH of the treated solution (de Mello Ferreira et al., 2013). With greater applied voltage, secondary reactions have also been observed, including hydrolysis at the anode to form oxygen gas (Arroyo et al., 2009; Bagga et al., 2008; Liu et al., 2010):

$$2\,H_2O \longrightarrow O_{2(g)} + 4\,H^+ + 4\,e^- \qquad \text{(Rxn 1.3)}$$

Such secondary reactions compete for current with the primary reaction at the anode (oxidative dissolution). Therefore, secondary reactions lower the Faraday efficiency of the reactor and are not typically favorable (Cataldo Hernández et al., 2012). If reactions 1.2 and 1.3 were the only favorable reactions, then the bulk pH would remain constant, because for every electron passing through the cell, one H^+ and one OH^- would be produced.

1.4.2 Aluminum and iron speciation

Aluminum and iron are the most common electrode materials used in electrocoagulation (Chen et al., 2000; Ozyonar & Karagozoglu, 2014; Dubrawski & Mohseni, 2013a; Behloul et al., 2013; Akbal & Camcı, 2012).

Reaction 1.1 applies to aluminum as follows:

$$\mathrm{Al} \longrightarrow \mathrm{Al^{3+}} + 3\,\mathrm{e^-} \qquad \text{(Rxn 1.4)}$$

Researchers have found that iron is oxidized to ferrous ions at the electrode surface (Bagga et al., 2008; Li et al., 2012).

$$\mathrm{Fe} \longrightarrow \mathrm{Fe^{2+}} + 2\,\mathrm{e^-} \qquad \text{(Rxn 1.5)}$$

Ferrous ions may then be oxidized to ferric ions by dissolved oxygen (DO) or other reactive species in solution (Li et al., 2012; van Genuchten et al., 2014; Wan et al., 2011).

$$\mathrm{Fe^{2+}} \longrightarrow \mathrm{Fe^{3+}} + \mathrm{e^-} \qquad \text{(Rxn 1.6)}$$

The latter reaction takes place by means of an intermediate oxidizing agent, modeled below as tetravalent iron:

$$3\,\mathrm{Fe^{2+}} + \mathrm{O_2} \longrightarrow \mathrm{FeO_2} + 2\,\mathrm{Fe^{3+}} \qquad \text{(Rxn 1.7)}$$

The intermediate oxidizing agent is immediately reduced by ferrous ions or other reductants in solution (Li et al., 2012).

Relative concentrations of ferrous and ferric ions are dependent on factors other than the presence of DO. Li et al. (2012) found pH to have a strong effect on iron oxidation, even within the pH range of natural waters. At pH 6.8, the concentration of Fe(II) increased linearly with reaction time and accounted for approximately 90% of total iron ions, whereas the Fe(II) fraction approached a steady concentration of approximately 2.5 mg/L at pH 7.6. In addition, charge loading rate (CLR), or the charge passed through

the cell per unit volume per unit time, influences iron oxidation. At low CLRs (*e.g.*, 1 C/L-min) the rate of ferrous iron oxidation approaches the rate of ferrous ion production by oxidative dissolution. At very low CLRs, electrolytic dissolution can be the rate-limiting reaction of Fe(III) formation (Wan et al., 2011). As CLR increases, ferrous ion production overtakes oxidation and results in a greater ratio of ferrous to ferric ions (Li et al., 2012). When present, natural organic matter (NOM) may chelate with and prevent oxidation of ferrous ions (Bagga et al., 2008). Finally, current density may limit iron oxidation by creating locally high concentrations of ferrous ions and low concentrations of DO at the anode surface (Cataldo Hernández et al., 2012). Conversely, current density may promote oxidation by mixing due to electrolytic gas evolution (Dubrawski & Mohseni, 2013b), or by increasing local pH (Bagga et al., 2008).

1.4.3 Coagulant formation

The metal cations form hydrated complexes in solution. These hydrated ions undergo hydrolysis to form metallic hydroxide species. For aluminum, the process is modeled as follows. Waters of hydration are omitted after the first two reactions for simplicity:

$$Al^{3+} + 6\,H_2O \longrightarrow Al^{3+}\cdot 6\,H_2O \qquad \text{(Rxn 1.8)}$$

$$Al^{3+}\cdot 6\,H_2O \longrightarrow Al(OH)^{2+}\cdot 5\,H_2O + H^+ \qquad \text{(Rxn 1.9)}$$

$$Al(OH)^{2+} \longrightarrow Al(OH)_2{}^{+} + H^+ \qquad \text{(Rxn 1.10)}$$

$$Al(OH)_2{}^{+} + H_2O \longrightarrow Al(OH)_{3(s)} + H^+ \qquad \text{(Rxn 1.11)}$$

$$Al(OH)_{3(s)} + OH^- \longrightarrow Al(OH)_{4(aq)}^- \qquad \text{(Rxn 1.12)}$$

Between pH 5 and 6, $Al(OH)^{2+}$ and $Al(OH)_2{}^{+}$ are the predominant mononuclear aluminum species. From pH 5.2 to 8.8, insoluble aluminum (III) hydroxide ($Al(OH)_3$) is predominant. Above pH 9, $Al(OH)_4{}^{-}$ dominates (Gomes et al., 2007). Aluminum solubility in a matrix modeled on natural waters is shown in Figure A.1, page 84. This more complex water matrix shows the prevalence of the aluminum hydroxide species in

solution, but also that $AlSO_4^+$ may become dominant below pH 5.5. Thus, the presence of sulfate ions can increase aluminum solubility below pH 5.5. An analogous transformation occurs with ferric ions, by which Fe^{3+} undergoes hydrolysis to form $Fe(OH)^{2+}$, $Fe(OH)_2^+$, $Fe_2(OH)_2^{4+}$, and others (Gomes et al., 2007). A solubility diagram of ferric iron is shown in Figure A.2, page 85. The dominant soluble species in the pH range of natural waters are $Fe(OH)_2^+$ below approximately pH 8, and aqueous $Fe(OH)_3$ and $Fe(OH)_4^-$ above pH 8. Only below pH 3 does $FeSO_4^+$ become prevalent. In comparision, ferrous ions are far more soluble (Bagga et al., 2008; Chen et al., 2000; Dubrawski & Mohseni, 2013a; Tanneru & Chellam, 2012), as shown in Figure A.3, page 85. Oxidation of ferrous ions is therefore critical for precipitation.

Both aluminum and ferric hydroxides precipitate between pH 6 and 9 (de Mello Ferreira et al., 2013). Iron (III) hydroxide is minimally soluble near pH 8 and aluminum hydroxide near pH 6.5 (Vepsäläinen et al., 2012), as shown in the solubility diagrams in Appendix A.1. However, even at pH 6.5, the concentration of soluble aluminum is over two orders of magnitude greater than that of ferric iron. Residual, soluble aluminum poses a potential problem for EC of potable water (Dubrawski & Mohseni, 2013a; Vasudevan & Lakshmi, 2011). The U.S. Environmental Protection Agency (EPA) provides non-enforceable, secondary standards of 0.05 to 0.2 mg/L (1.9 to 7.4 μM) for aluminum and 0.3 mg/L (5.4 μM) for iron. These secondary standards relate to color, odor and taste aesthetics for drinking water (US EPA, 2009). However, high concentrations of aluminum in drinking water have been linked to Alzheimer's Disease (Flaten, 2001).

In reality, myriad mono- and polynuclear oxyhydroxide species are created. The precise structure of the coagulant depends on numerous factors including pH, background electrolytes, temperature, DO and current density (Akbal & Camcı, 2012; Dubrawski & Mohseni, 2013a; Liu et al., 2010; Mouedhen et al., 2008; Parga et al., 2012). Aluminum hydroxides tend to form amorphous or very poorly crystalline structures such as γ' alumina (Gomes et al., 2007) with very large specific surface areas (Akbal & Camcı, 2012; Chen et al., 2000). Iron crystallization in solution varies greatly with reactor parameters and the water matrix (Dubrawski & Mohseni, 2013a; van Genuchten et al., 2014; Akbal & Camcı, 2012). A number of crystalline and pseudo-crystalline structures have been

identified from iron EC, such as magnetite (Fe_3O_4) and lepidocrocite (γ' FeOOH) (Dubrawski & Mohseni, 2013a; van Genuchten et al., 2014; Wan et al., 2011). Dubrawski & Mohseni (2013a) found that long residence times with high current density and DO availability gave rise to magnetite, whereas low DO and low current density gave rise to a loosely-defined compound called green rust (GR). Between extremes, loosely crystalline products (lepidocrocite and pseudo-lepidocrocite) are commonly formed (Dubrawski & Mohseni, 2013a; van Genuchten et al., 2014; Wan et al., 2011). In fact, to synthesize lepidocrocite in the lab (*e.g.*, for adsorption studies), ferrous iron is oxidized in the presence of DO at ambient temperature (Wan et al., 2011). Consisting of both ferric and ferrous hydroxides, with alternating positively and negatively charged layers, GR is an important intermediate in the Fe^0 oxidation, both in EC and in nature. Anions are incorporated into the structure as Fe^{2+} is oxidized to Fe^{3+}. This internal reactive area gives GR a very high specific surface area (Moreno et al., 2007). Highly crystalline species have smaller specific surface areas than amorphous species and therefore fewer sorption sites (Gomes et al., 2007). Sorbed contaminants may also affect the overall crystalline structure, as when arsenic and iron form the mineral scorodite ($FeAsO_4 \cdot 2\,H_2O$) by EC (Gomes et al., 2007; van Genuchten et al., 2014).

1.4.4 Metal adsorption and precipitation

Metal contaminants are removed by adsorption to flocs, precipitation and/or chemical transformation. Both aluminum and iron hydroxides have a strong affinity for charged metallic ions (de Mello Ferreira et al., 2013; Gomes et al., 2007; van Genuchten et al., 2014). Dissolved metal cations themselves complex with ligands like OH^- and precipitate (de Mello Ferreira et al., 2013). Contaminant ions and hydroxides may also co-precipitate by replacing ions in the floc matrix (Arroyo et al., 2009; Moreno et al., 2007). Metal hydroxide formation is most prevalent at high pH, so the region of elevated pH near the cathode may play an important role (de Mello Ferreira et al., 2013; Fernandes et al., 2014). Charged colloids, particles and ions are transported by the field between electrodes. The electrophoretic movement of negative charges to the anode and postitive

charges to the cathode helps to concentrate contaminant and coagulant species for greater contact (Parga et al., 2005).

Iron electrodes have been shown to promote redox transformations of metal oxoanions like arsenite and dichromate (Arroyo et al., 2009; Li et al., 2012). Dichromate ions may be reduced directly by ferrous ions generated at the anode (Arroyo et al., 2009):

$$\mathrm{Cr_2O_7^{2-}} + 14\,\mathrm{H^+} + 6\,\mathrm{Fe^{2+}} \longrightarrow 2\,\mathrm{Cr^{3+}} + 6\,\mathrm{Fe^{3+}} + 7\,\mathrm{H_2O} \qquad \text{(Rxn 1.13)}$$

Chromium (VI) reduction by ferrous ions and iron minerals like magnetite also occurs in the environment (Ellis et al., 2002). For reduced species like arsenite, the probable mechanism of oxidation is a transient iron oxidant formed during the O_2-mediated oxidation of ferrous ions (Li et al., 2012).

$$\mathrm{AsO_3^{3-}} + 2\,\mathrm{Fe^{4+}} \longrightarrow \mathrm{AsO_4^{3-}} + 2\,\mathrm{Fe^{3+}} \qquad \text{(Rxn 1.14)}$$

Direct oxidation and reduction of contaminants may also occur at the electrodes and in solution (Holt et al., 2005). However, evidence suggests that oxidation and reduction in bulk solution is far more important than contaminant transformations at the electrode surface (Noubactep, 2010).

1.5. Reactor operation

EC reactors are typically operated galvanostatically, *i.e.*, maintaining constant current, to allow simple calculation of charge. As mentioned earlier, CLR is charge per unit time per unit volume (*e.g.,* C/s-L); for constant current, CLR can be expressed as the current normalized for the treated volume (A/L) (Dubrawski & Mohseni, 2013b; Chen et al., 2000). CLR is the only variable parameter for most reactors and determines the rate of anode dissolution and electrolytic gas production (Dubrawski & Mohseni, 2013b; Liu et al., 2010). Current density (i) is the current per unit area. However, instead of referring to the area of the vector field between electrodes, current density in EC is taken

as the area of the reactive anode surface. Current density determines the flux of electrolytic gas bubbles and anodic cations. Equally crucial, current density determines the conditions of the microenvironment around the anode and cathode (*e.g.*, pH, advection and concentration gradients) (Cataldo Hernández et al., 2012; Liu et al., 2010).

As a matter of convenience, investigators typically choose to express results as functions of either CLR or current density. Many authors therefore tend to equivocate the two concepts, in that both CLR and current density are varied but results are attributed to one or the other. Chen et al. (2000), varied the cell current and volume flow rate in order to determine the effect of current density. The authors found that removal efficiencies for fats, oils and grease were affected by varying CLR, but not current density. However, increased current density requires greater applied voltage and therefore decreased power efficiency. At the same time, a low current density reactor must occupy a greater footprint (Chen et al., 2000; Vepsäläinen et al., 2012). Dubrawski & Mohseni (2013a,b) used a more robust approach by constructing a cell with replaceable baffles into which a varying number of electrodes could be inserted. By this method, current density could be altered without affecting the CLR or the flow of the cell. Lower current density was associated with greater removal efficiency of natural organic matter (NOM), the contaminant studied. For drinking water applications, a large electrode surface area (*i.e.*, low current density) may be preferential to reduce resistance across the electrolyte (ohmic dissipation), but flux of electrolytic gas bubbles would decrease. Lower bubble flux reduces mixing at the electrode surface and decreases removal by flotation (Dubrawski & Mohseni, 2013b; Cataldo Hernández et al., 2012; Liu et al., 2010).

To further confound the conversation, researchers often refer to CLR when assuming constant residence time. The operable variable in this case is coagulant dose normalized per unit volume, not CLR or residence time *per se*. The same specific dosage may be generated slowly by a low CLR and high residence time or quickly by a high CLR and low residence time. Dubrawski & Mohseni (2013a) analyzed each of these strategies and found that high CLR and low residence time enhanced flotation, while low CLR and high residence time allowed settling to occur. However, greater NOM removal efficiencies were found at lower CLRs, because a high CLR required either a higher coagulant dose or

post-treatment flocculation for maximum removal (Dubrawski & Mohseni, 2013b).

1.5.1 Power consumption

The power used by the reactor can be simply modeled as the product of the current and applied potential. In reality, the potential varies throughout galvanostatic reactor operation, so the parameters must be integrated over time. The applied potential required to maintain constant current is equivalent to the sum of three factors:

$$\eta_{AP} = \eta_k + \eta_{Mt} + \eta_{IR} \tag{1.3}$$

where η_{AP} is the applied overpotential (measured cell potential), η_k is the kinetic overpotential, η_{Mt} is the mass transfer overpotential and η_{IR} is the overpotential from ohmic dissipation, or IR drop. The kinetic, or activity, overpotential is the required potential to drive the numerous half-reactions that take place in the reactor, particularly for electrode dissolution and hydrolysis. Mass transfer, or concentration, overpotential is the added potential required to overcome localized depletion of charge-carrying ions near the electrode surface due to high reaction rates. Agitation from stirring or bubble flux can alleviate concentration overpotential (Liu et al., 2010; Cataldo Hernández et al., 2012). Ohmic dissipation can be reduced by increasing electrolyte conductivity, minimizing distance between electrodes or maximizing the area of the electrodes:

$$R = \left(\frac{1}{\kappa}\right)\left(\frac{l}{A}\right)_{effective} \tag{1.4}$$

where R is resistance, κ is the conductivity of the electrolyte, l is the distance between electrodes, and A is the cross-sectional area of the electric field. For large, plate electrodes spaced closely together, the cross-sectional area between electrodes approximates that of the electric field (Wright, 2007). By Ohm's Law, the theoretical applied voltage required to overcome the IR drop is the product of the current (I) and resistance (R):

$$V = IR \tag{1.5}$$

1.5.2 Post-treatment

EC treatment may be followed by gravitational separation as a clarification step. In many treatment conditions, flocs float to the surface, buoyed by electrolytic gas (Cataldo Hernández et al., 2012; Fernandes et al., 2014; Holt et al., 2005; Liu et al., 2010). This flotation layer can be skimmed from the surface as an alternate means of clarification. Several authors have also investigated EC in combination with membrane filtration, including reverse osmosis (Den & Wang, 2008), ultrafiltration (Ben-Sasson et al., 2011, 2013) and microfiltration membranes (Bagga et al., 2008; Ben-Sasson et al., 2011, 2013). Pretreatment of filtration source water by aluminum and iron EC has been shown to reduce membrane fouling (Ben-Sasson et al., 2011, 2013; Den & Wang, 2008), although a settling step between EC and filtration may be required (Bagga et al., 2008). In a field trial, Wan et al. (Wan et al., 2011) used a 1 μm filter after iron EC to remove arsenic from groundwater. The team found that filtration was necessary to reliably achieve removal below the Indian drinking water standard of 50 μg-As/L.

1.6. Effect of background electrolytes

Background electrolytes are those ions in the source water other than the contaminants of concern. In concert, electrolytes contribute to the ionic strength of the water and increase the solution conductivity. However, many electrolytes also have important individual effects on EC reactions.

1.6.1 pH

The solubility and speciation of coagulants is highly dependent on pH. Aluminum and ferric hydroxides are least soluble near and slightly above neutral pH (Arroyo et al., 2009; de Mello Ferreira et al., 2013). Likewise, many metal contaminants have decreased solubility in mildly basic environments (de Mello Ferreira et al., 2013; Fernandes et al., 2014). However, as pH transitions from acidic to basic pH, the surface charge of ferric and

aluminum oxides decreases from positive to negative, while contaminants with exchangeable hydrogen moieties (*e.g.*, $H_2AsO_4^-$) become more negatively charged. Thus, affinity decreases between negatively charged ions and coagulants (Li et al., 2012). pH also strongly affects the oxidation of not only ferrous iron (Li et al., 2012), but also redox transformations of contaminant species like chromium (VI) (Arroyo et al., 2009).

1.6.2 Hardness

van Genuchten et al. (2014) found that the presence of calcium and magnesium increased the size and density of iron flocs. The team also found that calcium and magnesium enhanced uptake of oxyanions (arsenate and phosphate) due to bonding between the cation and an oxygen from the anion.

1.6.3 Alkalinity

In a study of arsenic removal, Li et al. (2012) found that bicarbonate had no effect from 3 - 50 mM HCO_3^-. The presence of bicarbonate ions may encourage more ordered crystalline structures (*e.g.*, goethite) than found in poorly-adsorbing, monovalent electrolytes (van Genuchten et al., 2014).

1.6.4 Chloride

The presence of chloride accelerates both iron and aluminum dissolution by pitting corrosion (Arroyo et al., 2009; Mouedhen et al., 2008). Chloride ions have been also shown to be necessary for the formation of GR during EC (Dubrawski & Mohseni, 2013a; Moreno et al., 2007). Chloride also prevents the formation of a passivating oxide layer on aluminum electrodes. Passivation acts as an insulator on the electrode surface and increases the required potential and power consumption. Mouedhen et al. (2008) determined by potentiometric polarization that the minimum chloride concentration to prevent aluminum passivation was 60 mg/L (1.69 mM). de Mello Ferreira et al. (2013)

found no difference in electrode polarization curves between 0 and 5 mM chloride for current densities less than roughly 10 mA/cm^2. Therefore, below 5 mM chloride and 10 mA/cm^2, chloride should not significantly affect passivation or aluminum dissolution.

1.6.5 Sulfates

Sulfate has a low affinity for iron hydroxides and does not significantly affect contaminant removal or floc structure at natural concentrations (less than 200 mg/L) (Meng et al., 2002). Presumably for this reason, some researchers have used sulfate as a background electrolyte to maintain solution conductivity as other electrolyte concentrations are varied (de Mello Ferreira et al., 2013; Mouedhen et al., 2008).

1.6.6 Competing ions

Ions such as phosphate and silica reduce the number of available sorption sites for removal of the desired contaminant. Decreased sorption may be due to direct competition for sorption sites, as with phosphate (Li et al., 2012; van Genuchten et al., 2014; Wan et al., 2011), or restricted access to the internal surface area of the floc by polymeric structures on the floc surface, as with silica (Wan et al., 2011). As little as 1 mg/L phosphate has been shown to inhibit arsenic uptake (Wan et al., 2011), whereas silica may have negligible inhibition below relatively high concentrations (less than 36 mg/L) (Meng et al., 2002). Silica has also been shown to inhibit crystal formation by iron hydroxides (van Genuchten et al., 2014; Wan et al., 2011).

1.7. Heavy metal contamination in drinking water

1.7.1 Chromium

Chromium in natural waters exists in trivalent and hexavalent forms. While chromium (III) is an essential micronutrient, chromium (VI) is a highly toxic carcinogen

(Arroyo et al., 2009; World Health Organization, 2003a). The U.S. EPA specifies a Maximum Contaminant Level (MCL) for drinking water of 100 μg/L total chromium (US EPA, 2009). Chromium is generally not found in significant concentrations in uncontaminated, natural waters (World Health Organization, 2003a). Hexavalent chromium is used as a corrosion inhibitor and is found in wastewater from tanning, electroplating, wood preservation and mining and smelting. In the developed world, chromium discharge in wastewater is tightly controlled (Arroyo et al., 2009). Chromium (III) readily adsorbs to solids and complexes to form insoluble precipitates (Ellis et al., 2002; World Health Organization, 2003a), as shown near neutral pH in Figure A.4, page 86. As shown in Figure A.5, page 86, chromium (VI) remains soluble in pH ranges where chromium (III) precipitates. Therefore, reduction to chromium (III) not only reduces chromium toxicity, but also total chromium concentration.

1.7.2 Nickel

Nickel in drinking water arises primarily from plumbing, although natural sources and pollution from industries like nickel-cadmium battery manufacturing and electroplating may also be responsible. Though nickel may take on various valence states, aqueous nickel exists primarily as bivalent ions (Ni^{2+}) at environmental conditions. As shown in Figure A.6, page 87, presence of carbonate increases nickel solubility and leads to the formation of aqueous $NiCO_3$. Long-term ingestion of nickel may result in kidney or liver damage (World Health Organization, 2005). High nickel concentrations in drinking water have been linked to lung and bladder cancers in humans (Cantor, 1997). While the EPA does not regulate nickel in drinking water, the World Health Organization (WHO) advisory concentration for nickel is 70 μg/L (World Health Organization, 2005). The National Science Foundation/American National Standard Institute (NSF/ANSI) protocol for drinking water treatment units cites a maximum drinking water level (MDWL) of 100 μg/L nickel (NSF/ANSI, 2012).

1.7.3 Copper

Copper is a ubiquitous metal in electrical wiring, metallurgy, pesticides, electroplating, fertilizers, animal feed and numerous other uses (World Health Organization, 1996). A common contaminant in mine tailings (Lim et al., 2008), copper also enters the environment from printed circuit board manufacturing wastewaters (Cheung et al., 2003). Copper sulfate may be intentionally introduced to surface waters as an aquatic biocide (World Health Organization, 1996). Corrosion of household plumbing may also lead to unhealthy levels of copper in drinking water (US EPA, 2009). In water, copper typically forms bivalent ions (Cu^{2+}) (World Health Organization, 1996). Above pH 6, copper solubility drops off sharply and is primarily influenced by carbonate, as shown in Figure A.9, page 87. Copper in sediments is not stable and is likely to reenter the aquatic environment when pH decreases (Cheung et al., 2003).

Copper is an essential nutrient, with a recommended daily allowance of 900 μg/day for adults (World Health Organization, 1996). However, long-term ingestion of water with excessive copper can result in liver or kidney damage (US EPA, 2009). The action level specified by the EPA for copper in drinking water is 1.3 mg/L (US EPA, 2009).

1.7.4 Zinc

Zinc contamination in the environment arises from smelting, galvanization and diecasting industries (Cheung et al., 2003; Lim et al., 2008; Terres-Martos et al., 2002). Zinc contamination also arises from non-industrial sources like geologic deposits, household plumbing and solid waste leachate (Terres-Martos et al., 2002). When contaminated surface water is used for irrigation, zinc accumulates in soils and can then leach into the underlying groundwater (Terres-Martos et al., 2002). Soluble zinc between pH 6.5 and 8.5 occurs primarily as Zn^{2+} ions, although zinc also readily forms species with sulfate, carbonate and hydroxide ligands, as shown in Figure A.10, page 89. Like copper, residual zinc is likely to reenter solution when pH drops (Cheung et al., 2003). The EPA has a non-enforceable, secondary MCL of 5 mg/L zinc (US EPA, 2009).

1.7.5 Arsenic

Arsenic is a drinking water contaminant of high concern. Anthropogenic sources like mining and smelting, pesticide application and wood preservation contribute to arsenic contamination (Jarup, 2003). However, geologic sources of arsenic are very common worldwide. The earth's crust contains 1.8 mg/kg arsenic (Crittenden et al., 2013), and the rate of arsenic cycling in the environment is increasing due to human activity (Anawar et al., 2002). Arsenic deposits threaten drinking water supplies in the western United States, Mexico, Chile, Argentina, England, Hungary, Japan, China, India and Bangledesh (Anawar et al., 2002; Cantor, 1997; Jarup, 2003; Parga et al., 2005). Drinking water is the primary route of human exposure to inorganic arsenic (Jarup, 2003). In the U.S., 13 million people are exposed to arsenic levels above the EPA standard of 10 μg/L (Crittenden et al., 2013). Arsenic contamination in Bangladesh and West Bengal, India constitutes a humanitarian crisis and has been called the largest environmental disaster in human history (Anawar et al., 2002; Smith et al., 2000). Of Bangladesh's population of 125 million, an estimated 35 to 77 million people are at risk for arsenic poisoning from groundwater (Anawar et al., 2002; Smith et al., 2000).

Arsenic has both carcinogenic and non-carcinogenic toxicity (Anawar et al., 2002). No effective treatment is available for arsenic poisoning (Parga et al., 2005). Chronic arsenic ingestion results in skin lesions and cancer, internal cancers and diseases of the skeletal, neural and vascular systems (Cantor, 1997; Jarup, 2003; Smith et al., 2000). The World Health Organization (WHO) recommends a maximum drinking water concentration of 10 μg/L arsenic, and chronic ingestion of as little as 50 μg/L has been shown to cause precancerous lesions (Jarup, 2003; Smith et al., 2000). Groundwater arsenic concentrations in India and Bangladesh can range in the thousands of μg/L (Anawar et al., 2002; Cantor, 1997).

Though arsenic is a metalloid, it is often considered a heavy metal (Jarup, 2003). Arsenic speciation is highly dependent on environmental redox potential (Eh) and pH (Anawar et al., 2002; Crittenden et al., 2013). In natural waters, arsenic occurs primarily

as pentavalent arsenate (AsO_4^-) or trivalent arsenite (AsO_3^{3-}) (Gomes et al., 2007; Parga et al., 2005; Wan et al., 2011). At pH levels between 4 and 10, arsenite species are predominantly neutral, while arsenate is negatively charged (Crittenden et al., 2013; Parga et al., 2005), as shown in Figures A.11 and A.12, page 90. For this reason, arsenate more readily adsorbs and can be more easily removed than arsenite (Wan et al., 2011). Thus, oxidation is generally considered a required pre-treatment for arsenite mitigation (Crittenden et al., 2013; Wan et al., 2011). At a high redox potential, arsenite is readily oxidized to arsenate at any pH (Gomes et al., 2007). Arsenite exists in significant concentrations under anaerobic conditions (as in groundwater), while arsenate is prevalent in surface waters with high DO concentrations (Crittenden et al., 2013; Parga et al., 2005).

1.7.6 Cadmium

Cadmium contamination arises from electroplating and the manufacture of rechargeable nickel-cadmium batteries (Cheung et al., 2003; Jarup, 2003). Cadmium is also used industrially as a pigment, a stabilizer in PVC, a by-product of fuel combustion, and an anti-corrosive. However, most cadmium released to the environment comes from non-ferrous metal smelting. Chronic ingestion of low levels of cadmium leads to kidney damage or failure, as well as skeletal deterioration. Cadmium is also likely to increase risk of cardiovascular disease and death and is classified as a human carcinogen (Jarup, 2003). The MCL for cadmium in drinking water is 5 μg/L (US EPA, 2009). Cadmium has been detected in surface water and sediments at high levels downstream of mining operations (Cheung et al., 2003; Lim et al., 2008). Near neutral pH, Cd^{2+} ions dominate, as shown in Figure A.13, page 91. Given sufficient chloride concentration, $CdCl^+$ ions are also prevalent. Cadmium solubility dips between pH 8 and 12. The majority of cadmium in sediments is stable and unlikely to become bioavailable (Cheung et al., 2003).

1.7.7 Lead

Though most developed countries have banned the use of tetraethyl lead in gasoline, "leaded" gasoline remains a major source of lead contamination internationally (Cheung et al., 2003; Jarup, 2003). Lead enters surface waters from both urban runoff and the settling of lead in auto exhaust (Cheung et al., 2003; Jarup, 2003). Other sources of lead are mines and smelting, glass and battery manufacture, and geologic deposits (Lim et al., 2008; Jarup, 2003; US EPA, 2009). In the developed world, lead contamination in drinking water often comes from corrosion of residential plumbing (US EPA, 2009). Lead is acutely poisonous, and chronic exposure can lead to kidney damage. Lead is also a potential human carcinogen. Inorganic lead passes through the blood-brain barrier in children but not adults. Thus, chronic exposure is more hazardous to children and leads to permanent behavior, learning and concentration disorders (Jarup, 2003). The EPA specifies an action level for lead in drinking water of 15 μg/L (US EPA, 2009), while the WHO specifies an advisory concentration of 10 μg/L (World Health Organization, 2003c).

1.7.8 Current methods of heavy metal removal

Conventional removal of metal contaminants from water involves chemical precipitation, such as lime softening; sorption or filtration, such as granular media filtration; ion exchange (IX); and reverse osmosis (RO). Chemical precipitation requires bulk chemical inputs up to twice the stoichiometrically determined mass, produces a high volume of sludge and generally only reduces contaminants to the part per million level (Akbal & Camcı, 2012; Daous & El-Shazly, 2012; Dermentzis et al., 2011). As seen in the previous sections, many metal contaminants have drinking water limits in the low parts per billion. Therefore, chemical precipitation is likely inadequate to achieve drinking water standards.

Granular media filtration and lime softening can be effective in removing arsenate, chromic ions, copper and lead, but are not effective against chromate and arsenite. Novel sorbents such as granular ferric hydroxide and activated alumina have also been

investigated for arsenic removal. Despite successful trials, such sorbents are cost-prohibitive, work in a narrow pH range and require pre-oxidation of arsenite (Crittenden et al., 2013).

IX is effective against charged ions like arsenate, chromic ions, chromate, copper and lead. However, uncharged species like arsenite are not removed by IX, and a single medium will only remove either anions or cations (Crittenden et al., 2013). In addition, exchange media require expensive chemical or physical regeneration (Dermentzis et al., 2011; García-Lara et al., 2009). RO provides the most consistent removal of heavy metals and does not require pre-oxidation of arsenite (Crittenden et al., 2013). However, removing metals to ultra-low concentrations entails high energy and membrane replacement costs (Garcia et al., 2013).

1.8. Electrocoagulation for heavy metal removal

Several authors have investigated EC for removing heavy metals from industrial wastewaters (Akbal & Camcı, 2012; Arroyo et al., 2009; Dermentzis et al., 2011; Li et al., 2014). In wastewaters, operators may increase conductivity and prevent electrode passivation by addition of salts (de Mello Ferreira et al., 2013). In addition, typical metal concentrations and regulatory limits are far higher for wastewater than drinking water.

Relatively few authors have considered EC for water potabilization. Initial results indicate that EC can achieve removal of nickel, copper, zinc, chromium and arsenic to below regulatory levels (Cataldo Hernández et al., 2012; de Mello Ferreira et al., 2013; Li et al., 2012; García-Lara et al., 2009). Most studies of EC in potable water have tested removal of contaminants from a natural water source. Cataldo Hernández et al. (2012) tested a 400 mL batch reactor with aluminum plate electrodes for removal of very low levels of nickel and chromium from two groundwater sources in Italy. After 120 minutes treatment at a charge density of 0.8 to 1.6 mA/cm^2, nickel concentrations were lowered from 41 to 22 μg/L, and chromium from 23 to 20 μg/L. In another study, de Mello Ferreira et al. (2013) tested copper, nickel and zinc removal from Grenoble tap water. The team used relatively high initial concentrations (12 mg Cu/L, 20 mg Zn/L, 20 mg Ni/L).

After 60 minutes of treatment at 1 A (1.4 mA/cm^2), all three metals were removed by 95%. Ratna Kumar et al. (2004) tested arsenic removal from tap water. Iron electrodes achieved near 100% removal of arsenite with approximately 250 C/L charge loading, or 86 mg/L coagulant dose. Arsenate was also shown to temporarily rise at the beginning of treatment, indicating that arsenite was oxidized prior to removal. García-Lara et al. (2009) used a continuous flow reactor to treat Mexico groundwater containing 133 μg/L total arsenic (10.5 μg/L arsenite) and found removal to below 10 μg/L arsenic after two minutes of treatment at a flow rate of 0.875 L/min and current density of 3 mA/cm^2. Air was sparged in the reactor at a rate of 1.6 L/min for mixing and to encourage arsenic and iron oxidation.

At least two field trials have been conducted on arsenic removal from groundwater by EC. Parga et al. (2005) used a pilot-scale, mobile EC unit (Lamar Mobil Pilot Plant) with iron and carbon steel electrodes to remove arsenic from Mexico groundwater. The pilot plant had a flow rate of 30 L/min and was operated at 4 to 5 A and 20 to 40 V, with injected air sparging. After a 90 second residence time, total arsenic was reduced from 2.24 mg/L to 5 μg/L. The unit's energy expenditure was estimated to cost 0.2 cents per cubic meter treated. In a field trial in West Bengal, India, Wan et al. (2011) distributed household EC units to 17 homes. The units used iron electrodes, aquarium pumps for air sparging, with post-treatment filtration by 1 μm filters. Households used the units for one week to treat groundwater containing an average of 400 μg/L arsenic with a treatment time of 3 hours. The units used approximately 0.75 kWh/m^3 water treated, or about \$0.11 in local costs. The team also found that 3 units were not used properly, indicating that training is integral for the success of low-tech, point-of-use units.

Other investigators have used simple electrolytes to better characterize the fundamental mechanisms behind EC. Mouedhen et al. (2008) tested removal of high concentrations of zinc, nickel and copper (67, 59 and 67 mg/L, respectively) from a sodium sulfate and sodium chloride electrolyte with an initial pH of 4.9. All three metals were removed 40 to 60% after 20 minutes at 0.25 A (5 mA/cm^2) and 100% after 75 minutes. In another test of EC in synthetic water, Nouri et al. (2010) showed zinc and copper removal from a 1.6 mS/cm potassium chloride electrolyte. The team found greater

than 90% removal near neutral pH after 15 minutes of treatment at 30 V, but decreasing removal efficiency with lower initial concentrations (from 500 to 5 mg/L). Gomes et al. (2007) tested arsenic removal in sodium chloride electrolyte and reduced arsenic concentration from 1.42 mg/L to less than 0.10 mg/L after 60 minutes of treatment at 30 mA/cm^2. Li et al. (2012) created a synthetic groundwater for testing. The team used a reactor with iron electrodes (1 to 24 C/L-min CLR) and found reduction in arsenic concentration from 500 μg/L to below 50 μg/L. The team found a pattern of a temporary, initial increase in arsenate concentration, as also noted by Ratna Kumar et al. (2004).

1.9. Research goal

The research in this study is unique in that it addresses seven different metal contaminants at the trace concentrations of concern to human consumption. In addition, this study investigates the wide range of possible source water compositions. Most research of metal contaminant removal by EC has used contaminant concentrations and water matrices applicable to wastewater but not potable water. To date, the few studies of EC treatment of drinking water have focused on a single metal or small suite of contaminants. The wide range of operating parameters makes comparison between studies difficult. In addition, research to date has used either a single natural water source or simple electrolyte solutions. Thus, the wide variation in natural waters has not been examined. As described above, electrolytes in the water matrix, such as calcium, magnesium, bicarbonate and chloride ions, have the potential to radically influence floc formation, contaminant removal and power consumption. In addition, post-treatment with microfiltration may provide additional contaminant removal compared to settling or flotation.

The overarching goal of this study was to determine the feasibility of aluminum and iron EC to remove trace heavy metals from a wide range of drinking water sources. This work was carried out in accordance with three specific objectives:

Objective 1: Demonstrate removal of contaminants to below regulatory levels.

The first objective of this study was to investigate whether EC can remove contaminant metals to regulatory levels (MCLs or secondary standards) established by the U.S. EPA. In the first phase of tests, individual metal contaminants were tested for removal based on NSF/ANSI protocol for drinking water treatment units. Maximum removal of each contaminant metal was sought. To this end, very high coagulant doses were used to bypass potential restabilization by charge reversal and ensure removal by sweep flocculation. The second phase of tests sought to show simultaneous removal of a cocktail of contaminant metals. One potential benefit of EC over IX would be simultaneous removal of both anions (*e.g.*, arsenate and dichromate) and cations (*e.g.*, divalent nickel, cadmium and lead ions). Contaminant metals were expected to show poorer removal in mixed-contaminant tests than in single-contaminant tests due to competition for sorption sites.

Objective 2: Determine the effects of reactor design on metal removal.

The second objective was to determine the effects of major reactor design choices on contaminant metal removal. Specifically, the use of iron or aluminum electrodes and post-treatment settling or microfiltration were investigated. To this end, aluminum and iron electrode performance was compared through a series of repeated tests using solutions of mixed contaminants. After EC, samples were treated by microfiltration or settling alone. Iron was expected be more effective than aluminum in removing arsenic and chromium when spiked as arsenite and dichromate, respectively, due to iron's ability to drive redox transformations. Iron was also expected to benefit most from filtration, based on initial observations that iron electrodes formed smaller, less dense flocs than aluminum electrodes.

Objective 3: Determine the effects of the gross water matrix on metal removal.

The final objective was to determine the effects of influent water quality on contaminant metal removal. Instead of varying a single background ion or using a single natural water, four synthetic waters were created to represent the ionic composition of a wide range of natural waters, as described in Section 2.2. Of these four representative waters, two were tested at two different pH levels.

Poorer contaminant removal was expected with increasing chloride, sulfate and carbonate anion concentrations due to increased metal speciation and solubility, as well as competition for sorption sites. Divalent cations (Ca^{2+} and Mg^{2+}) were expected to generally decrease removal by disrupting the coagulant matrix and reducing floc surface charge by substitution. For iron electrodes, EC was expected to achieve greater arsenic removal in high hardness waters due to Ca-O-As complexation (van Genuchten et al., 2014).

Cadmium and lead were expected to show the greatest removal at high pH due to low solubility, as shown in Figures A.13 and A.14, pages 91 and 91. Also, iron was expected to outperform aluminum at pH 8.5. Iron (III) is minimally soluble near pH 8.5, as shown in Figure A.2, page 85, whereas aluminum is minimally soluble below pH 6.5, as shown in Figure A.1, page 84. However, because low pH promotes oxidation of ferrous ions to ferric ions (Li et al., 2012), iron was also expected to perform better at pH 6.5 than pH 8.5.

2. METHODS

2.1. Reactor design and operation

Electrocoagulation tests were conducted in a bench-scale, batch reactor with a retention volume of 300 mL. The reactor was constructed of plastic and was stirred at 60 rpm with a magnetic stir bar measuring 5 cm long and 0.8 cm in diameter. Plate electrodes consisting of aluminum or iron (>90% purity) were used for both the anode and cathode. Each electrode had a submerged surface measuring 9 x 6 x 0.3 cm (115 cm^2 effective surface area). The inter-electrode distance was 1 cm. Power was supplied by a 330 W DC power supply (Sorensen LH 110-3) with a constant current of 0.50 A (100 C/L-min CLR, 4.3 mA/cm^2 current density). The electrode polarity was alternated every 30 seconds to prevent electrode passivation. The reactor apparatus, electrodes and polarity-alternating controller were kindly provided by A.O. Smith Water Products Company. Initial and final applied potential readings were taken from the digital reading on the power supply. Power consumption (P) in watts was estimated as the product of the constant current (I_c) in amperes and mean applied potential ($\bar{V}$) in volts:

$$P = I_c \bar{V} \tag{2.1}$$

2.2. Test water formulation

Contaminant removal was tested in synthetic waters. Four different synthetic test waters were prepared by spiking ultrapure (Milli-Q) water with American Chemical Society (ACS) grade reagents to approximate major ion concentrations in representative source waters. The pH was adjusted to desired levels by addition of hydrochloric acid or sodium hydroxide. The test waters modeled the low and high range of ionic concentration for both surface and groundwater. Thus, the progression from lowest to highest total dissolved solids (TDS) was as follows: “surface low,” “surface high,” “ground low,” and “ground high,” as shown in Table 2.1.

Table 2.1: Synthetic test waters and range of water quality parameters investigated.

Test Water	pH	TDS (mg/L)	Hardness	Guidance
Surface low	6.5, 8.5	160	60	NSF/ANSI 53:2011
Surface high	6.5, 8.5	300	120	
Ground low	6.5	880	370	Snoeyink & Jenkins, 1980
Ground high	6.5	2,110	470	Delhi test well

The reagents and quantities used to formulate each test water are provided in Appendix A.2, page 93. "Surface low" and "surface high" test waters were formulated to represent a range of surface water conditions based on parameters for metal contaminant removal conditions required by NSF/ANSI 53:2011a (NSF/ANSI, 2012). However, to allow comparison between metals, two composite surface waters were created to approximate many of the different "challenge" waters for individual metals outlined in the NSF/ANSI protocol. In addition, the low solids water outlined by the protocol was not a realistic candidate for treatment by EC due to the very low (< 100 mg/L) TDS concentration stipulated. The extremely low conductivity of the water specified in the protocol required over 100 V of applied potential to pass 0.5 A of current, and initial tests showed that the water heated to 35°C within minutes. Thus, "surface low" was modeled to require less than 50 V applied potential based on Equation 1.4, page 13, and Ohm's Law (Equation 1.5, page 13), while aligning as closely as possible to the characteristics outlined in NSF/ANSI 53:2011a.

"Ground low" test water was modeled on well water in Dayton, Ohio, as characterized in Snoeyink & Jenkins (1980). "Ground high" test water was modeled on brackish water from a well in Delhi, India. Sampling data for the well was provided by A.O. Smith Corporation. For each test water, calcium and magnesium hardness, bicarbonate alkalinity and sulfate concentrations were matched as closely as possible to the source water. Reproducing these concentrations in the lab at standard temperature and pressure required an excess of chloride and sodium ions above reported concentrations. These excesses were as follows: "surface low", 0.8 mM chloride and 0.7 mM sodium; "surface high," 1.6 mM chloride and 1.7 mM sodium; "ground low," 5.4 mM chloride and 5.2 mM sodium; and "ground high," no excess chloride or sodium. Given the current density used in this study (4.3 mA/cm^2), absolute chloride concentrations below 5 mM should not affect electrode polarization (de Mello Ferreira et al., 2013). "Ground low" slightly exceeded this level (5.6 mM Cl^-). "Ground high" greatly exceeded 5 mM chloride but matched the chloride concentration found in the brackish Delhi well (18.9 mM Cl^-).

Metal contaminants were spiked into the water at the challenge concentrations established in NSF/ANSI 53-2011a, as shown in Table 2.2, page 30. Nickel and zinc were

not addressed in NSF/ANSI 53-2011a. For these metals, spiking concentrations were chosen to ensure solubility while exceeding regulatory limits by a factor of at least 3.

Table 2.2: Spiking concentrations and target concentration levels for the seven metal contaminants of interest.

Species	Spiking Compound	Influent challenge concentration (μg/L as element)	U.S. EPA Maximum contaminant level (MCL) (μg/L as element)
As	$AsNaO_2$	300	10
Cd	$CdCl_2$	30	5
Cr	KCr_2O_7	300	100
Cu	$CuCl_2 \cdot 2\,H_2O$	3,000	1,300
Ni	$NiCl_2 \cdot 6\,H_2O$	500	100[a], 70[b]
Pb	$Pb(NO_3)_2$	150	10
Zn	$ZnCl_2$	15,000	5,000[b]

a Maximum Drinking Water Level (MDWL), NSF/ANSI 53:2011a

b WHO advisory concentration, not MCL

2.3. Chemical equilibrium modeling

Speciation of coagulant and contaminant metals was modeled in each of the four test waters with MINEQL+, version 4.6. Metal solubilities were modeled assuming the potential to form all species provided in MINEQL+. Thus, the calculated solubilities are conservative and may be higher in reality due to non-equilibrium conditions. Speciation diagrams are for metals at the spiking concentrations in Table 2.2 in "ground high" water, unless otherwise specified. Initial concentrations above 10 M were not allowed by the program. Therefore, the solubility of ferrous iron could only be modeled above pH 5.

2.4. Post-treatment and analysis

After EC treatment, the flotation layer (if present) was removed with a pipet. The bulk solution was then stirred gently to homogenize and transferred to 50 mL centrifuge tubes. In the interest of time, settling by gravitation was simulated by centrifugation for 5

minutes at 2,910 *x g*. These centrifugation parameters were similar to those described by Matsui et al. (2003). The supernatant was then decanted. Approximately half of the supernatant was next filtered through a dead-end, 0.45 μm cellulose nitrate filter. Filtration was performed using a vacuum manifold (approximately 50 kPa gauge). To ensure metal solubility for analysis, 50 mL samples of both the permeate (microfiltered) and the supernatant (settled only) were digested on a hot plate with 5 mL concentrated nitric acid according to Standard Method 3030 E (American Public Health Association et al., 1998). Sample volumes were reduced to approximately 10 mL, then reconstituted in Milli-Q water. Samples were then diluted for analysis in a solution of 2% OmniTrace Ultra nitric acid (EMD Millipore #MNX0408) and 0.5% Aristar Ultra hydrochloric acid (BDH #20401) for metals analysis. Dilution factors were chosen to achieve less than 5 mg/L total analyte concentration. In all tests, iron or aluminum was the limiting analyte in determining appropriate dilutions. For this reason, lower coagulant doses allowed for less dilution and thus improved the method detection limits (MDLs, see Section 2.8).

Metal concentrations were analyzed by inductively coupled plasma mass spectrometry (ICP-MS, Agilent 7700 series) according to Standard Method 3120 B (American Public Health Association et al., 1998). An AS X-500 ICP-MS auto-sampler was used. The instrument blanks consisted of 2% nitric, 0.5% hydrochloric acid as described above. An internal standard mix of bismuth, germanium, indium, lithium, scandium, terbium and yttrium (Agilent #5183-4681) was used throughout the analysis. Samples were calibrated and analyzed with Mass Hunter Workstation software, version B.01.01.

2.5. Phase 1: single-contaminant removal

Metal removal was addressed in two distinct phases. In the first phase, removal of each of seven metal contaminants was tested separately. These contaminants were chromium, nickel, copper, zinc, arsenic, cadmium and lead. The first objective of these tests was to show removal of contaminants to below regulatory levels. Therefore, retention times of 15, 30 and 60 minutes (1500, 3000 and 6000 C/L, respectively) were chosen.

These operating conditions exceed typical coagulant doses, but allowed evaluation of maximum contaminant removal. Samples were taken only at the end of each test, not continuously during EC treatment. A single test was run for each retention time. The second objective was to determine operating conditions, particularly CLR and retention time. In this phase, two test waters were used: "surface low" and "surface high." "Surface low" was tested at pH 6.5, and "surface high" was tested at pH 8.5, as outlined by the challenge conditions for metal removal provided in NSF/ANSI 53-2011a (NSF/ANSI, 2012).

2.6. Phase 2: mixed-contaminant removal

In the second phase, the removal of metal contaminants was tested simultaneously using mixed solutions of five metals (chromium, nickel, arsenic, cadmium and lead). Zinc and copper were not included in this phase, because the high spiking concentrations of the two metals influenced the solubility of the remaining species. The reduction of metal solubility was shown both by equilibrium modeling and experimentally in the lab. Upon addition of all seven metals in solution, a bright yellow precipitate formed that was easily removed by filtration. The remaining five metals did not significantly influence the solubility and speciation of the others, as evidenced by metal concentrations in filtered samples and equilibrium models shown in Figures A.4 - A.14, pages 86 - 91.

Four independent variables were tested in this phase: electrode material (aluminum or iron), post-treatment (microfiltration or settling alone), initial pH and test water type. Triplicate tests were performed for each test condition. The retention time was held constant at 2 minutes (200 C/L) for all tests. This retention time was chosen to ensure less than 50 mg/L of total analytes in all samples, based on concentrations found in previous tests. After a 10x dilution, all samples would then meet the required maximum concentration of 5 mg/L total analytes for ICP-MS analysis. A 10x dilution was chosen to achieve MDLs appreciably lower than the regulatory limits (see Section 2.8).

Metal removal efficiency in all four test waters was tested in this phase. Mixed contaminant removal in "surface low" and "surface high" waters was tested at both pH

6.5 and pH 8.5. "Ground low" and "ground high" waters were tested only at pH 6.5. According to equilibrium modeling, lead solubility at pH 6.5 varies considerably with carbonate concentration, as shown in Figure A.15, page 92. As the difference in lead solubility between pH 6.5 and 8.5 was greatest for the high solids waters, the surface waters were chosen to test at two pH levels. Other metals did not show pronounced differences in solubility between waters in the pH range tested. Ground waters were tested at pH 6.5 to ensure solubility of all metals at the initial, spiking concentrations.

2.7. Data analysis

In determining the effectiveness of EC treatment, both the post-treatment concentrations and removal efficiency for each metal were considered. The removal efficiency ($\eta_{removal}$) for each contaminant was calculated as follows:

$$\eta_{removal} = 1 - \frac{C_{post-treatment}}{C_{initial}} \tag{2.2}$$

The initial concentration ($C_{initial}$) was measured in the pre-treatment, filtered sample, and the post-treatment concentration ($C_{post-treatment}$) was measured in the microfiltered and unfiltered samples after EC. Thus, removal was calculated based solely on the initial concentration of dissolved metal in solution.

Comparisons of the resulting removal efficiencies (means of triplicate tests in the second phase of metal testing) were performed using four-way (multivariate) analysis of variance (ANOVA) tests to determine the effects of four, categorical independent variables: water matrix composition, pH, electrode material and post-treatment (settling versus microfiltration). Removal efficiency for each metal was first analyzed as a full matrix of two-, three- and four-way interactions between variables. Interactions with conservatively low significance ($p > 0.10$) were then disregarded and pooled into the error term. Type III sum of squares was used for all tests. Significant effects for each combination of independent variables were checked for normality using the one-sample Kolmogorov-Smirnov test and homogeneous variance using the Bartlett test. Where

groups with significantly different means were non-normal and/or heteroscedastic, data were transformed using the Box-Cox method and analyzed again by ANOVA. ANOVA assumptions of normality and homoscedacity were again checked for the transformed results. Because only two of the four test waters ("surface low" and "surface high") were tested at different pH levels, testing pH alongside the other variables could result in non-rank comparisons. Where a non-rank or heteroscedastic groups showed a significant interaction (*e.g.*, pH x test water), the data were divided into groups by the relevant variable(s) and reanalyzed by ANOVA to determine significant effects of remaining variables within those groups. Where data are displayed in "box and whisker" plots within this paper, whiskers represent the full range of data up to 1.5 times the interquartile range (1.5 IQR rule). The effect of electrode material on power consumption was analyzed by comparing mean applied potential for aluminum and iron in each test water using a two-tailed, paired t-test. All analyses were performed in MATLAB®, version R2013b.

2.8. Quality control

Reactors and all glassware were cleaned in a 5% hydrochloric acid bath and rinsed four times with Millipure water. Solution pH was adjusted in the reactor to ensure that any residual acid would not affect pH. Electrodes were polished before each test with 400 grit, waterproof, silicon carbide sandpaper under tap water to remove any adherent metals and ensure a uniform surface. Electrodes were then wiped clean and triple-rinsed with Milli-Q water. "Blanks" were sampled from each batch of test water prior to spiking with contaminant metals. Blank samples were subjected to the same pretreatment and analysis as experimental samples. Blank concentrations were not subtracted from the experimental concentrations because metals were frequently removed to near the blank concentrations. Instead, method detection limits (MDLs, 99% confidence) were determined from analyte concentrations in the blanks, as shown in Table 2.3, page 35. MDLs were calculated by the following formula for a series of single analyses:

$$MDL = s_s t \sqrt{\frac{n+1}{n}} \tag{2.3}$$

where s_s is the standard deviation of blank samples, t is the critical t-value ($p = 0.01$, two-tailed), and n is the number of samples (Sawyer et al., 2003).

Table 2.3: Method detection limits (MDLs, in μg/L) for the seven metal contaminants of interest by sample dilution.

Dilution:	10 X			20 X			100 X		
Metal	s_s	n	MDL	s_s	n	MDL	s_s	n	MDL
Cr	3.24	10	11.0	4.11	8	14.4	6.34	11	21.0
Ni	45.0	10	153	153	8	535	1,160	11	3,840
Cu	33.9	10	116	5.82	8	20.4	227	11	751
Zn	136	10	464	110	8	385	3,180	11	10,500
As	1.54	10	5.26	n.d.*	8	n.d.*	1.22	11	4.03
Cd	0.831	10	2.83	0.802	8	2.81	4.48	11	14.8
Pb	1.36	10	4.64	4.05	8	14.2	24.5	11	81.1

* Arsenic was not detected (< 0.001 μg/L) in blanks at this concentration.

3. RESULTS AND DISCUSSION

3.1. Coagulant dose

The rate of coagulant dosing was tested using aluminum and iron electrodes at 2 minutes and 15 minutes of treatment at 0.50 A. "Surface high" water was used as the supporting electrolyte. The Faraday efficiency for each metal was determined according to Equation 1.2, page 5. The dosing rate for aluminum was 3.96 mg/min (0.147 mmol/min), with a Faraday efficiency of 142%. Faraday efficiencies for aluminum in excess of 100% have been reported, and likely arise from chemical degradation of electrodes (*e.g.*, by pH or chloride) in addition to electrolytic degradation (Mouedhen et al., 2008; Kuokkanen et al., 2013). Iron had a similar dosing rate by mass – 3.07 mg/min (0.055 mmol/min) – but a much lower Faraday efficiency of 35.4%. Previous authors reporting high Faraday efficiencies (approaching 100%) for iron have used high chloride electrolytes and washed electrodes with acid to remove iron bound to the electrode surface (Dubrawski & Mohseni, 2013a). This experiment was concerned with the available coagulant throughout the reactor rather than the mass balance of iron, so the low Faraday efficiency is not a concern. In addition, the difference in molar dosing between aluminum and iron is of secondary concern to the performance of each electrode material for a given CLR and retention time. In optimizing an EC reactor for contaminant removal, these operating parameters are of greater importance. The reaction stoichiometry can inform as to the dissolution rate of the electrodes.

3.2. Aluminum and iron residuals

After two minutes of treatment with aluminum electrodes, microfiltered samples contained an average of 0.42 mg/L aluminum (standard deviation (SD) = 0.53, $n = 17$), while centrifuged samples contained an average of 3.05 mg/L ($SD = 2.21$, $n = 16$). After two minutes of treatment with iron electrodes, microfiltered samples contained an average of 0.35 mg/L iron ($SD = 0.55$, $n = 18$), while centrifuged samples contained an average of

4.45 mg/L ($SD = 4.20$, $n = 18$). Given these averages across all test conditions, both residual aluminum and iron exceeded secondary standards for drinking water of 0.2 and 0.3 mg/L, respectively (US EPA, 2009). Iron exceeded the standard by an average of 0.05 mg/L, while aluminum exceeded the maximium standard by a factor of 2.

Grouping the results by initial pH paints a different story, however. At pH 6.5, residual aluminum concentrations averaged 0.11 mg/L ($SD = 0.059$, $n = 12$) in filtered samples, versus 1.15 mg/L ($SD = 0.37$, $n = 5$) in filtered samples at pH 8.5. On the other hand, filtered iron samples at pH 8.5 contained less residual iron ($M = 0.043 mg/L$, $SD = 0.010$, $n = 6$) than at pH 6.5 ($M = 0.50 mg/L$, $SD = 0.62$, $n = 12$). Unfiltered samples showed the same trends by pH, but no division of unfiltered samples met the secondary MCLs for aluminum or iron.

Whereas the secondary standard for iron is an aesthetic limit (US EPA, 2009), chronic ingestion of aluminum in drinking water has been linked to Alzheimer's Disease (Flaten, 2001). Iron levels above 0.3 mg/L may discolor laundry and plumbing, but humans ingest far more iron in food (10 to 14 mg/day on average) than in drinking water (World Health Organization, 2003b). Therefore, slightly elevated levels of iron in drinking water are of little health concern. Microfiltration reduced both iron and aluminum concentrations by approximately one order of magnitude.

3.3. Objective 1: Contaminant removal

In the first, exploratory phase of metal contaminant testing, reduction to below the MCL was observed for the most toxic metals, as shown in Figures 3.1 - 3.7, pages 39 - 43. In these initial tests, aluminum and iron electrodes showed similar performance, with the notable exceptions of chromium and arsenic. Chromium, copper and cadmium were reduced to below the MCL within 15 minutes (1,500 C/L) with both aluminum and iron electrodes. Iron electrodes achieved greater removal of both chromium and arsenic. Arsenic was reduced to below the MCL within 15 minutes using iron electrodes but required 60 minutes of treatment (6,000 C/L) using aluminum electrodes.

At the dilution required for ICP-MS analysis, both nickel and zinc had MDLs in

excess of the target metal concentrations. For this reason, a reduction to the MCL could not be shown. Because nickel and zinc were spiked at high levels compared to other contaminants, the error likely arose from contamination rather than instrument limits. Contamination may have been introduced from the lab environment and digestion acids, despite acid washing reactors and glassware. The electrodes themselves contained impurities that may have been introduced into solution by electrolysis. In the first phase, lead was spiked at too high a concentration due to gross error. However, as reduction to below the MCL was shown in the second phase of metal testing, these tests were not repeated.

The first phase showed that metal removal to low μg/L levels was possible for the metals of highest toxicity – arsenic, chromium and cadmium – as well as copper. In addition, the results from the first phase served to determine an appropriate retention time for further investigation into the effect of reactor and water quality parameters on metal removal. Even in the challenging, mixed-contaminant conditions in the second phase of testing, chromium, arsenic, cadmium and lead showed repeatable (95% confidence) removal to below the MCL for some test conditions after only two minutes (400 C/L), as shown in Figures 3.8 - 3.16, pages 45 - 66.

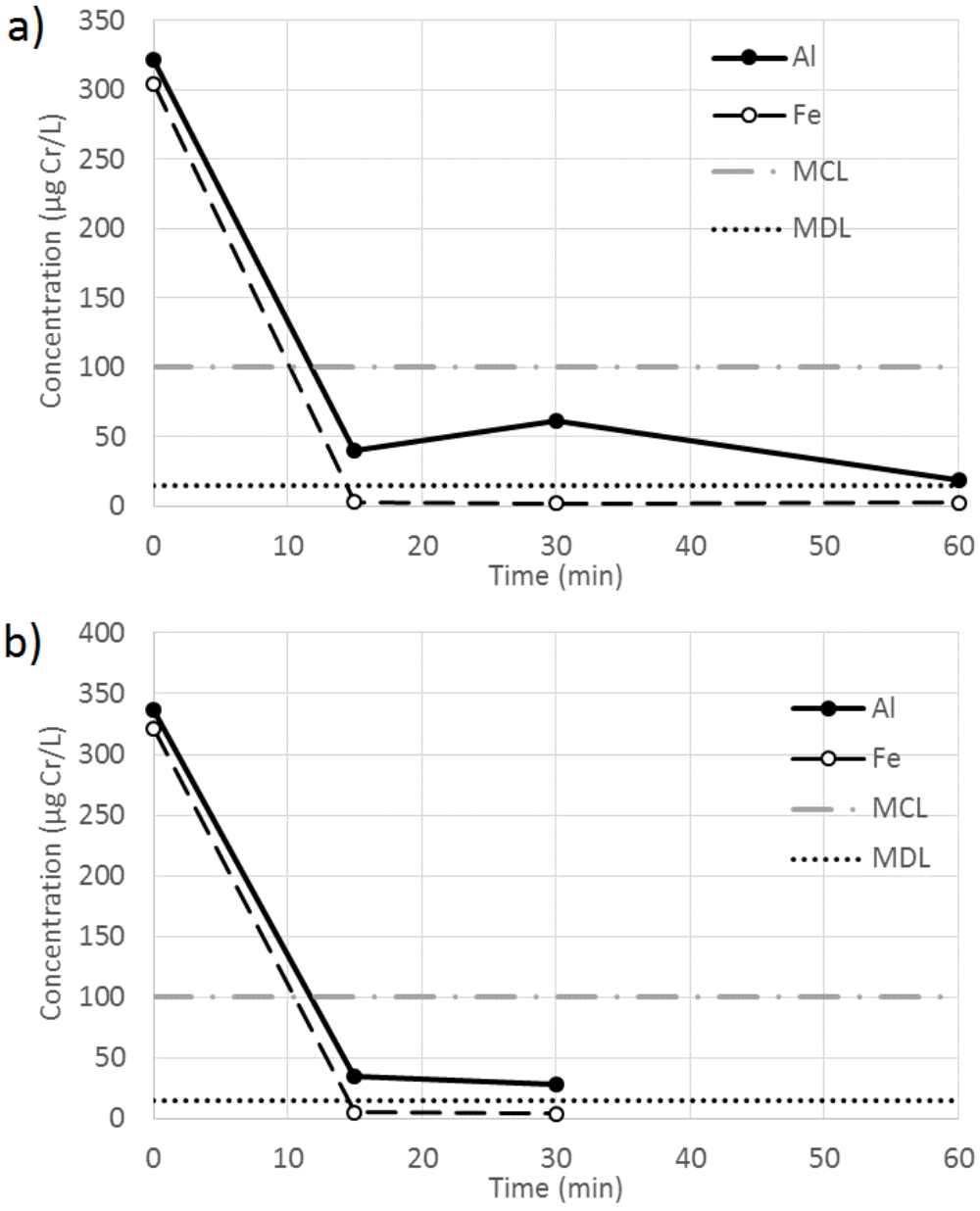

Figure 3.1: Chromium removal by aluminum and iron electrocoagulation, a.) pH 6.5, and b.) pH 8.5. Data points for each retention time represent individual tests.

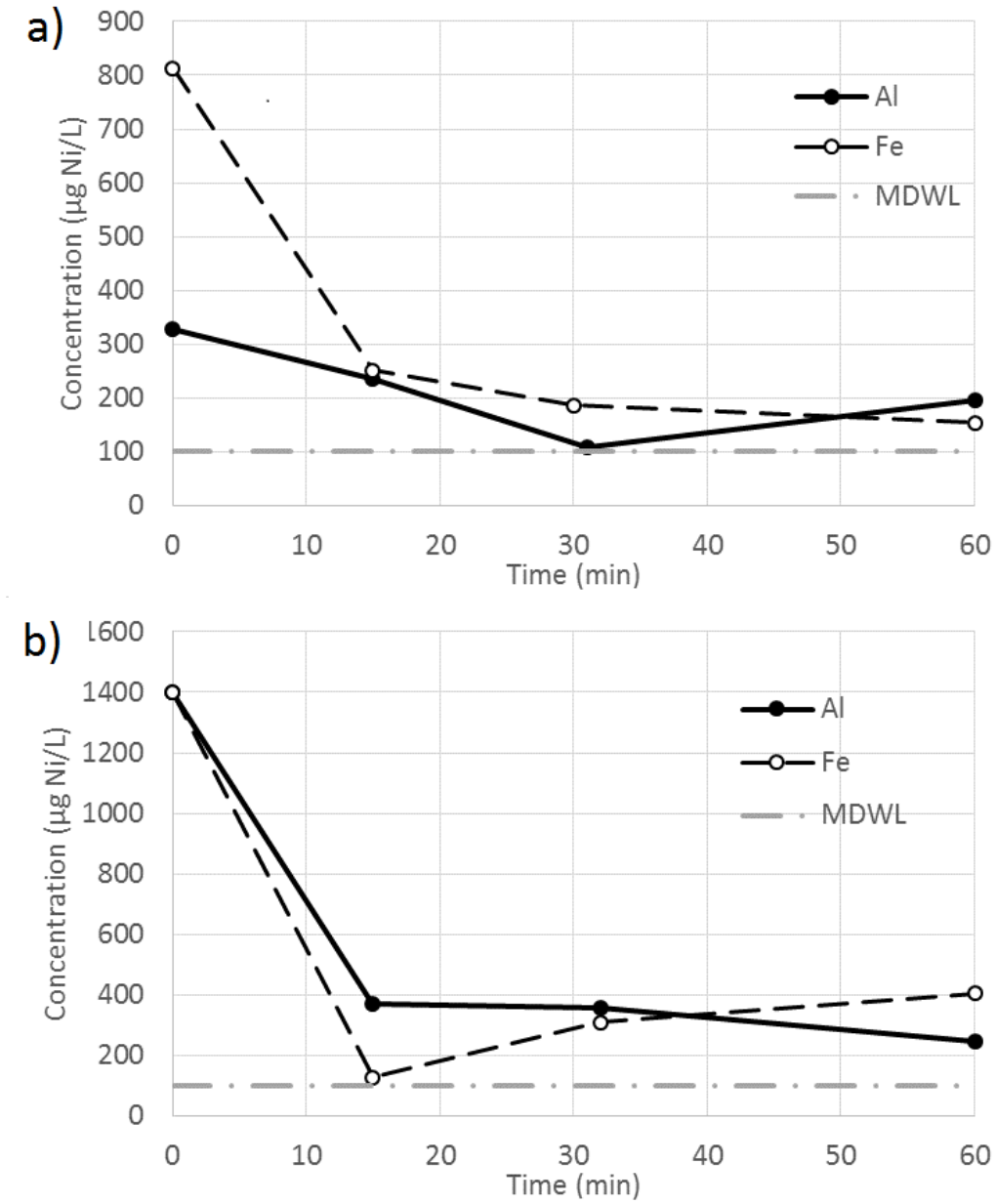

Figure 3.2: Nickel removal by aluminum and iron electrocoagulation, a.) pH 6.5, and b.) pH 8.5. Data points for each retention time represent individual tests. Due to sample dilution, the MDL for nickel ($3,840$ μg/L) was higher than the initial spiking concentration and is not shown in this figure. In b), the slight increase in concentration after 15 minutes with iron electrodes is likely due to chance variation between tests.

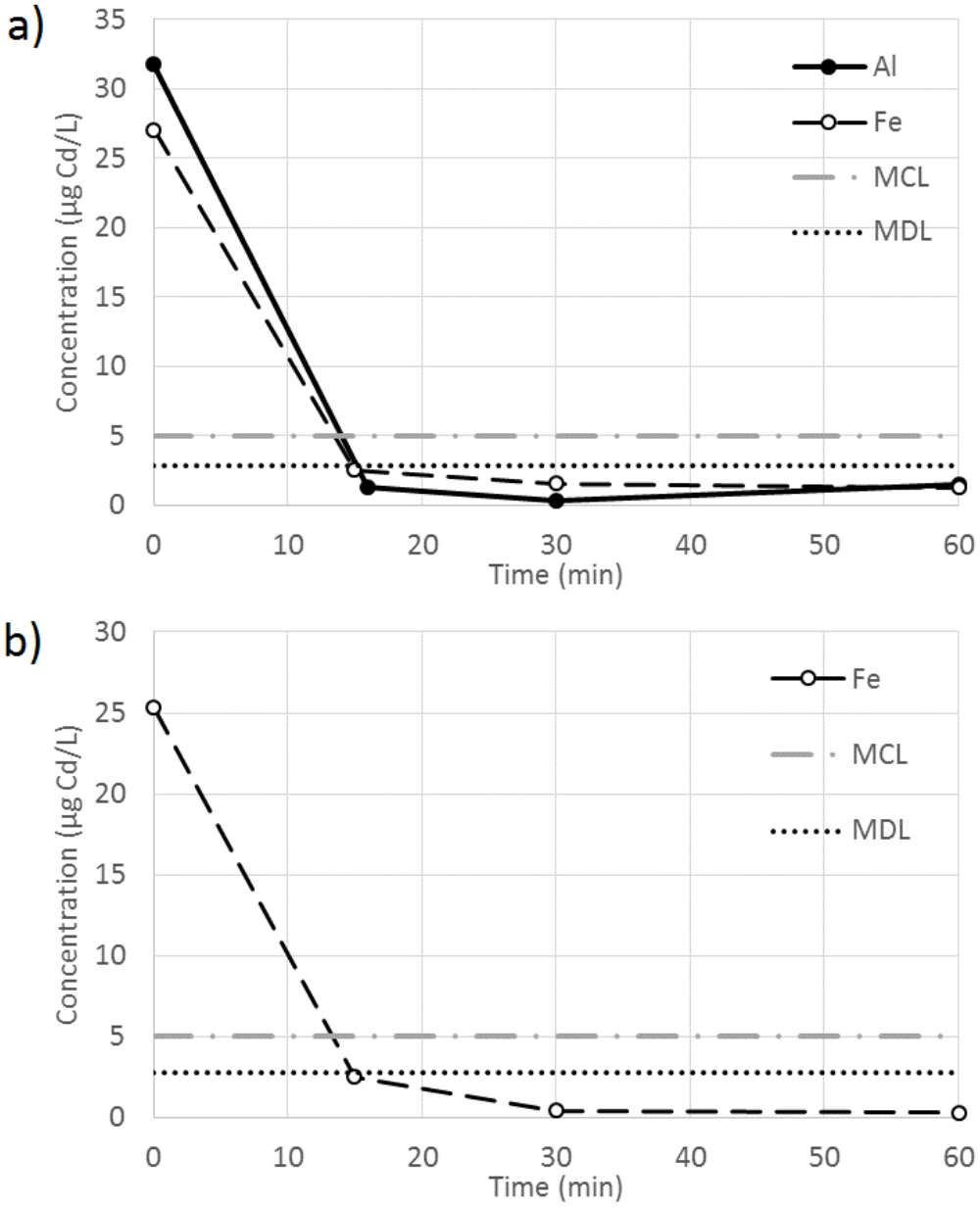

Figure 3.3: Cadmium removal by iron electrocoagulation, a.) pH 6.5, and b.) pH 8.5. Data points for each retention time represent individual tests. Aluminum electrodes were not tested at pH 8.5 due to the similar removal of both electrode materials at pH 6.5.

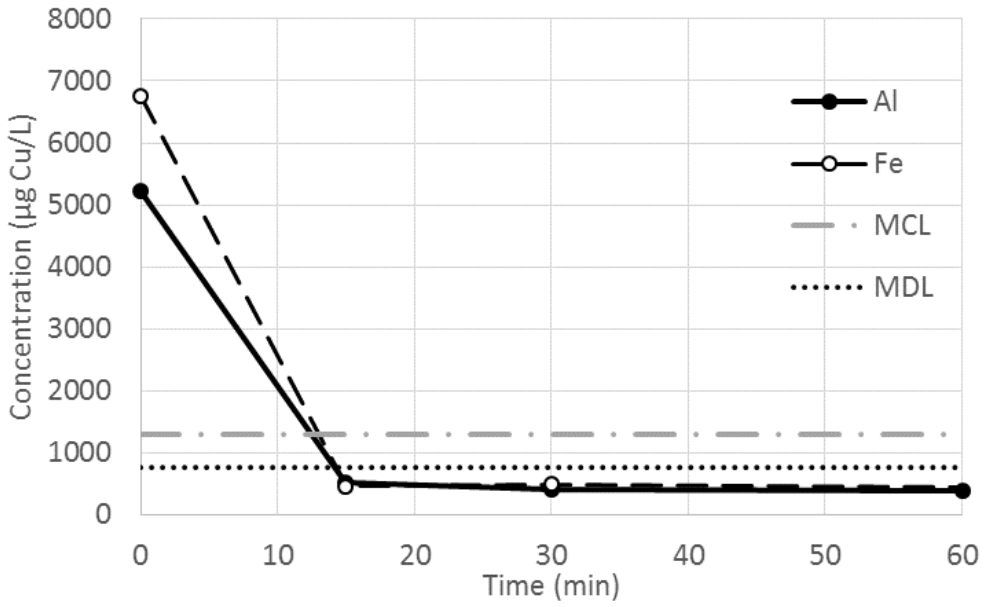

Figure 3.4: Copper removal by aluminum and iron electrocoagulation, pH 6.5. Data points for each retention time represent individual tests.

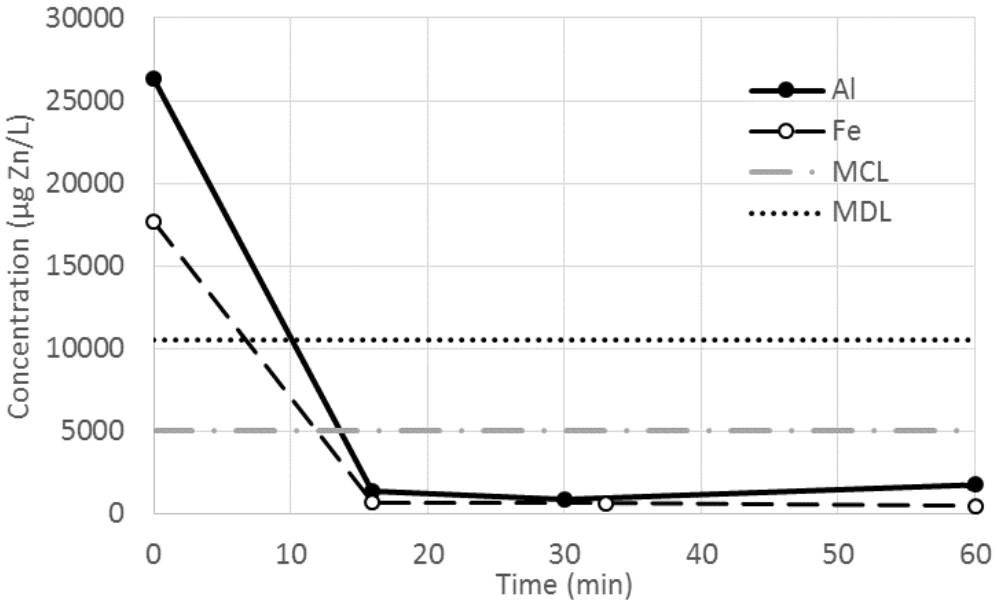

Figure 3.5: Zinc removal by aluminum and iron electrocoagulation, pH 6.5. Data points for each retention time represent individual tests.

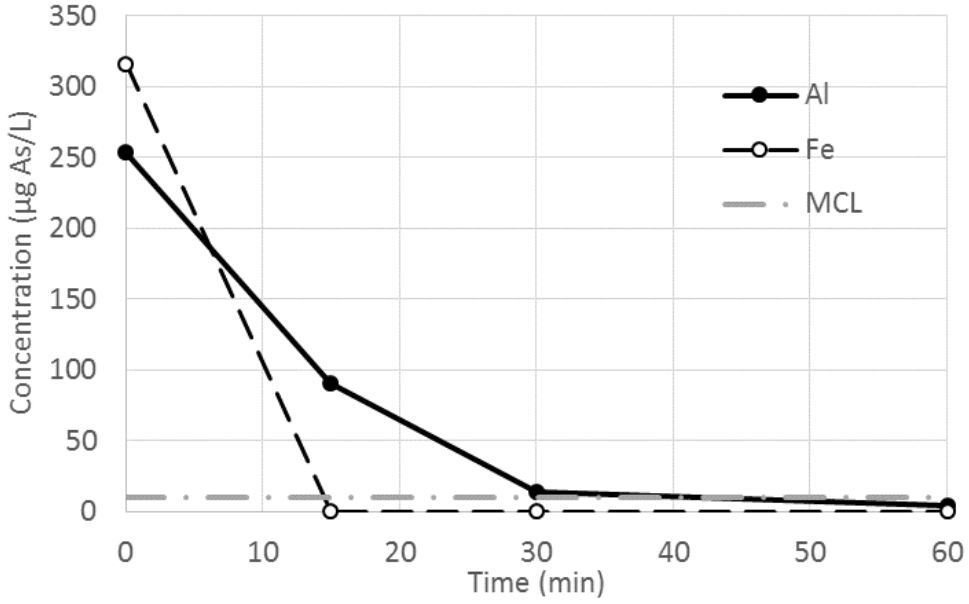

Figure 3.6: Arsenic removal by aluminum and iron electrocoagulation, pH 6.5. Data points for each retention time represent individual tests. Blank samples at this dilution (x20) showed no measurable concentration of arsenic, so the MDL was not calculable.

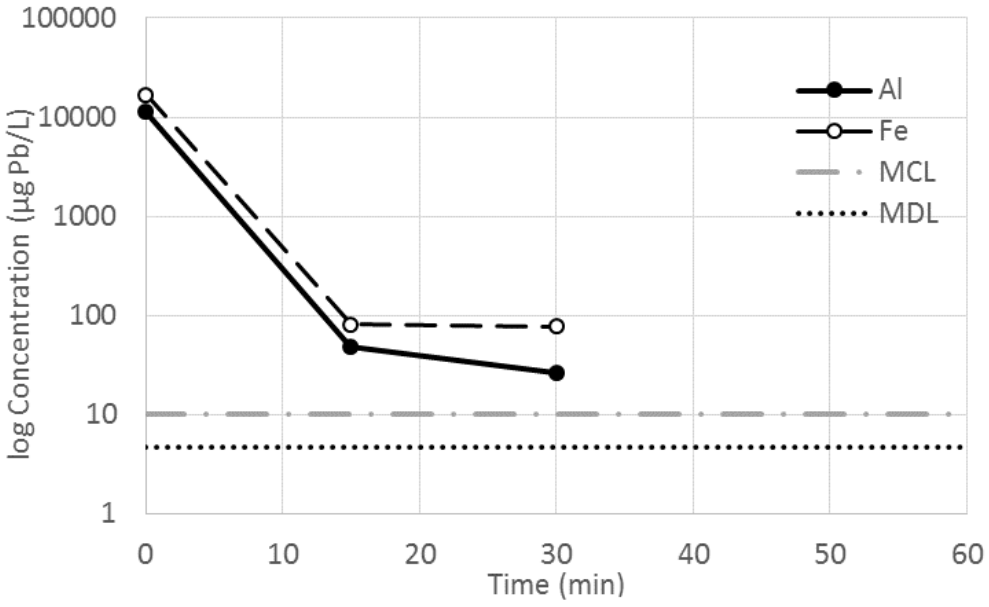

Figure 3.7: Lead removal by aluminum and iron electrocoagulation, pH 6.5. Data points for each retention time represent individual tests.

3.4. Effects of reactor and water matrix parameters by metal

This section discusses how the four independent variables tested in Phase 2 (electrode material, post-treatment, pH and test water type) affect the removal of each metal contaminant. Metal contaminants are considered individually to show the process of data analysis. The emphasis in this section is on determining significant effects and explaining those effects with regard to each metal contaminant. To that end, only the relevant figures and tables will be presented to illuminate how significance was demonstrated. The following Sections 3.5 and 3.6 synthesize the results in this section and discuss the broad trends in reactor and water matrix variables.

3.4.1 Chromium

The results for chromium removal in Phase 2 are shown in Figure 3.8, page 45. Chromium removal efficiency was compared between test conditions by 4-way ANOVA. Chromium removal efficiency in each test was tranformed using the Box-Cox method to correct for normality and homogeneous variance. Where post-treatment concentrations were slightly higher than the corresponding filtered, initial concentration, the resulting removal efficiency was negative. Therefore, unity (1) was added to all removal efficiencies before transformation to yield only positive values, because the Box-Cox transformation does not allow negative values. Significant effects ($\alpha > 0.05$) were shown for all four independent variables: post-treatment ($F(1, 59) = 11.11$, $p = 0.0015$), pH ($F(1, 59) = 6.99$, $p = 0.011$), test water ($F(3, 59) = 9.05$, $p = 0.0001$), and electrode material ($F(1, 59) = 805.5$, $p < 0.0001$). In addition, significant interactions were shown for electrode material and each of the remaining three variables: electrode x post-treatment ($F(1, 59) = 7.75$, $p = 0.0072$), electrode x pH ($F(1, 59) = 5.27$, $p = 0.025$), and electrode x test water ($F(3, 59) = 6.87$, $p = 0.0005$). Even with transformed data, the distribution of all filtered samples and all samples at pH 6.5 were determined to be non-normal by the Kolmogorov-Smirnov test. Post-treatment and pH were tested again by nonparametric, Kruskal-Wallis ANOVA. By Kruskal-Wallis, post-treatment was determined to be

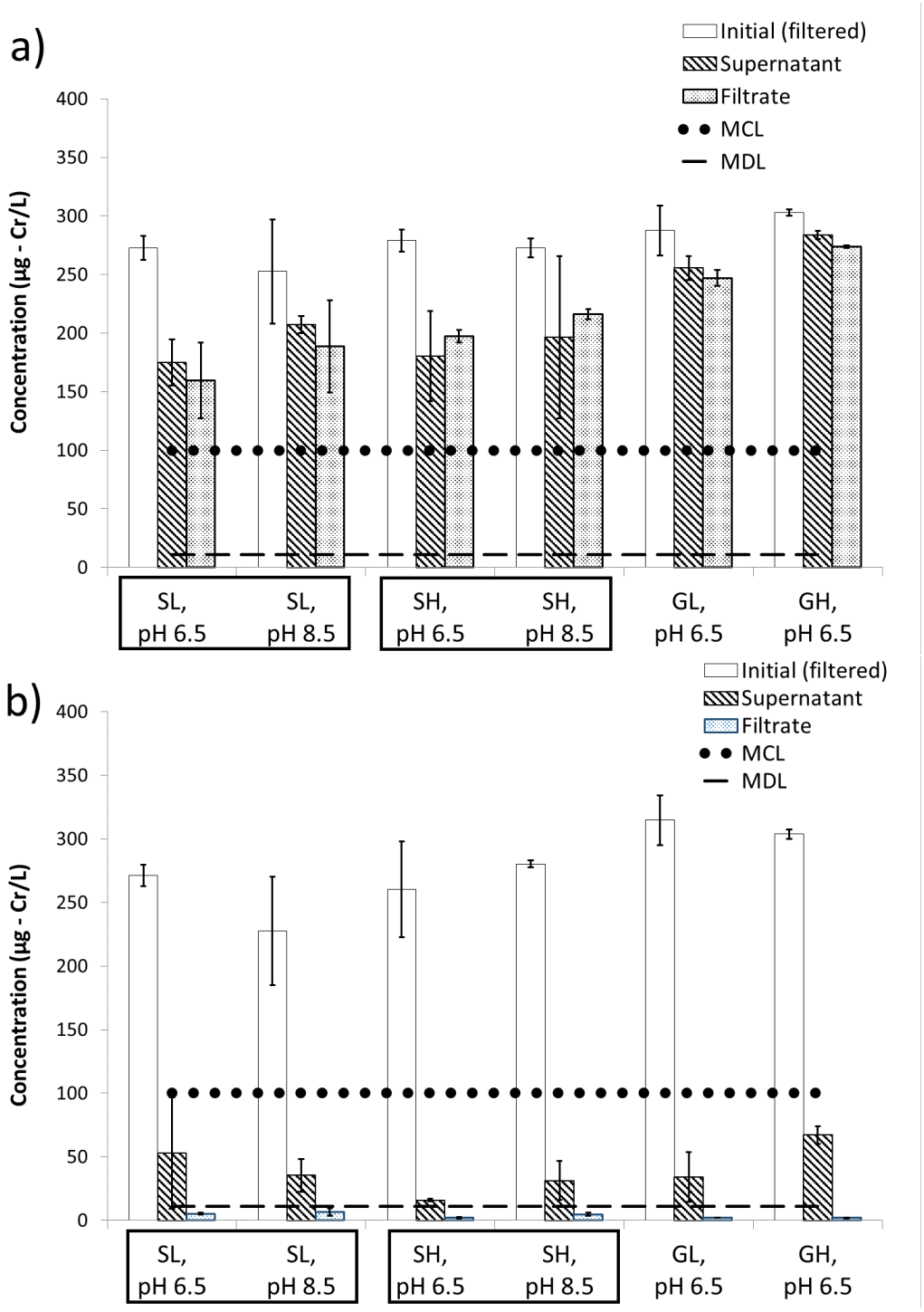

Figure 3.8: Chromium removal by a.) aluminum, and b.) iron electrocoagulation in six synthetic water matrices spiked with mixed contaminants. Note the dramatic removal of chromium with iron electrodes compared to that with aluminum electrodes. Test water types were abbreviated as follows: SL ("surface low"), SH ("surface high"), GL ("ground low"), GH ("ground high"). See Section 2.2 for a description of the four test water types. Values shown are means of triplicate tests; error bars are ±1 standard deviation.

significant ($X^2(1, 69) = 3.96$, $p = 0.047$), but pH was not ($X^2(1, 69) = 0.15$, $p = 0.69$).

Data grouped by electrode material failed to meet the assumption of equal variance for ANOVA. Grouping data by electrode material and any other variable(s) did not result in sets of equal variance either. The source of unequal variance (heteroscedacity) can be clearly seen in Figure 3.9, page 48. With iron electrodes and post-treatment microfiltration, chromium saw repeatable, near-complete removal, regardless of test water or pH. Because the data cannot spread past 100% removal, the variance was compressed. Despite failing the assumption of homoscedacity, electrode material clearly had a significant effect on chromium removal, given the comparatively poor performance of aluminum electrodes, the very low probability of the difference between electrode materials occurring by chance (as determined by ANOVA), and the fact that the narrow variance resulted from consistently excellent removal. Even so, the data were grouped by post-treatment, and the group receiving only settling was compared by three-way ANOVA (pH, test water and electrode material). In the subset of settled samples, Box-Cox transformations of the data resulted in homoscedastic, normal distributions. Significant effects were found for test water ($F(3, 29) = 4.61$, $p = 0.0094$) and electrode material ($F(1, 29) = 274.7$, $p < 0.0001$).

Chromium removal efficiency with iron electrodes (mean (M) = 0.92, $SD = 0.090$) was drastically greater than with aluminum electrodes ($M = 0.23$, $SD = 0.15$). The extreme difference in electrode performance explains the large standard deviations across other variables when lumping together results for aluminum and iron electrodes. Iron was expected to perform better than aluminum, as previous authors had postulated that ferrous iron released at the anode reduces dichromate ions in solution (Arroyo et al., 2009).

In general, chromium removal was significantly enhanced by microfiltration ($M = 0.61$, $SD = 0.39$) over settling alone ($M = 0.55$, $SD = 0.35$). However, enhancement from microfiltration was evident only for iron electrodes, as shown in Table 3.1, page 48. This electrode by post-treatment interaction agrees with observations that iron flocs were smaller and less dense than aluminum flocs. Iron particles often remained in suspension after centrifugation or became re-suspended with the slightest movement.

Chromium removal efficiency was greatest in low-solids waters: from “surface low”

($M = 0.61$, $SD = 0.34$) and "surface high" ($M = 0.62$, $SD = 0.35$), to "ground low" ($M = 0.53$, $SD = 0.43$) and finally "ground high" ($M = 0.48$, $SD = 0.43$). However, due to consistently high chromium removal with iron electrodes regardless of other variables, the trend is only apparent for aluminum electrodes, as shown in Table 3.2, page 49. Though pH was not shown to be have a significant effect, the mean removal efficiency was greater at pH 6.5 ($M = 0.642$, $SD = 0.309$) than pH 8.5 ($M = 0.585$, $SD = 0.379$) when comparing data from surface waters alone. Given the failure of the Kruskal-Wallis test to confirm the significance of pH and the relatively minor difference in group means, pH was not a relevant factor over the range tested.

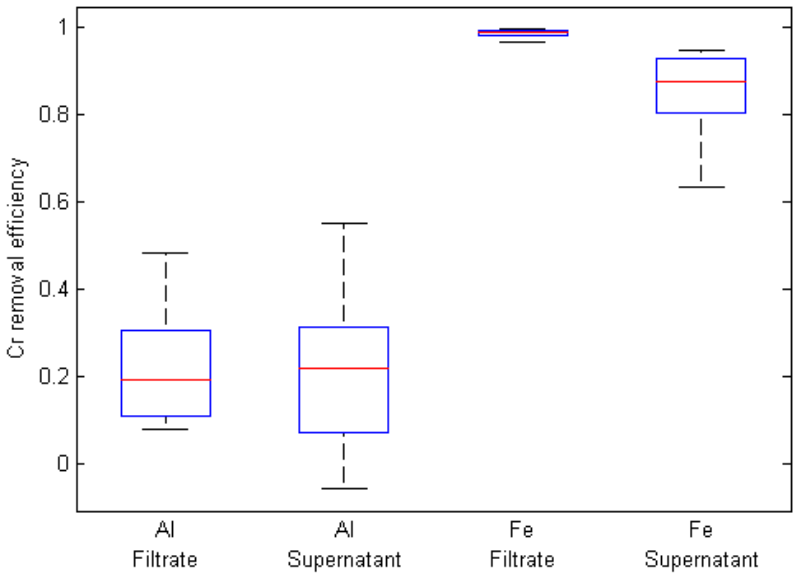

Figure 3.9: Chromium removal efficiency by treatment with aluminum versus iron electrodes, and post-treatment microfiltration versus settling only. Note that the samples treated by iron EC and microfiltration show very little variation due to nearly complete removal.

Table 3.1: Chromium removal efficiency, interaction between post-treatment and electrode material. Microfiltration significantly enhanced removal of chromium with iron electrodes, but not with aluminum electrodes.

		Electrode Material	
Post-treatment		Aluminum	Iron
Settling			
	n	17	18
	M	22%	86%
	SD	17%	8.8%
Microfiltration			
	n	18	18
	M	23%	99%
	SD	13%	0.88%

Table 3.2: Chromium removal efficiency, interaction between test water and electrode material, pH 6.5. Only data from pH 6.5 is shown to avoid confounding the effect of water matrix with the effect of pH on the two surface waters. EC with aluminum electrodes shows a clear trend of decreasing chromium removal with increasing ionic strength of the electrolyte from "surface low" to "ground high". Iron does not show the same trend, possibly due to consistently excellent removal.

		Electrode Material	
Test water		Aluminum	Iron
Surface Low			
	n	6	6
	M	39%	89%
	SD	7.9%	14%
Surface High			
	n	6	6
	M	32%	97%
	SD	11%	3.0%
Ground Low			
	n	6	6
	M	13%	94%
	SD	3.8%	7.0%
Ground High			
	n	6	6
	M	8.0%	89%
	SD	2.1%	12%

3.4.2 Nickel

ANOVA analysis of nickel removal efficiency showed significant effects for pH ($F(1, 63) = 100.1$, $p < 0.0001$) and test water ($F(3, 63) = 7.18$, $p = 0.0003$). In addition, results showed a significant interaction between pH and electrode material ($F(1, 63) = 10.82$, $p = 0.0016$). However, groundwater tests showed significantly lower variation than tests in surface water, as shown in Figure 3.11, page 53. Separating groundwater tests by other significant variables and combinations of variables did not resolve the difference in variation. In addition, transformations did not reduce the heteroscedacity. Aluminum flocs were observed to be larger in groundwater than surface water tests. Regardless of electrode material, flocs in groundwater may have been larger, denser and more likely to be removed consistently by settling and filtration. Groundwater tests were performed last chronologically, and the test methods had likely grown more consistent as well. Were nickel solubility lower in surface waters over the pH range tested, kinetic differences in precipitate formation could make nickel removal more variable in surface waters. Based on equilibrium modeling, nickel should remain soluble at the spiked concentration between pH 6.5 and 8.5, regardless of the test water used. A comparison of solubility in the four test waters is shown in Figure A.7, page 87. Therefore, differences in nickel solubility between waters is unlikely to result in the difference in variation.

The results for nickel removal in Phase 2 are shown in Figure 3.10, page 51. Due to the heteroscedacity between surface water and groundwater tests, the results for surface waters and groundwaters were analyzed separately. In surface waters, nickel removal showed significant effects from pH, as well as an interaction between pH and electrode type. The Kolmogorov-Smirnov test showed that results for aluminum electrodes at pH 6.5 were non-normal due to a single outlier. When this outlier was removed, pH ($F(1, 40) = 92.79$, $p < 0.0001$) and the pH x electrode material interaction ($F(1, 40) = 13.16$, $p = 0.0008$) remained significant, but the groups were no longer homoscedastic. Transformations did not correct for non-normality or heteroscedacity. The complete surface water data for the four combinations of electrode material and pH were

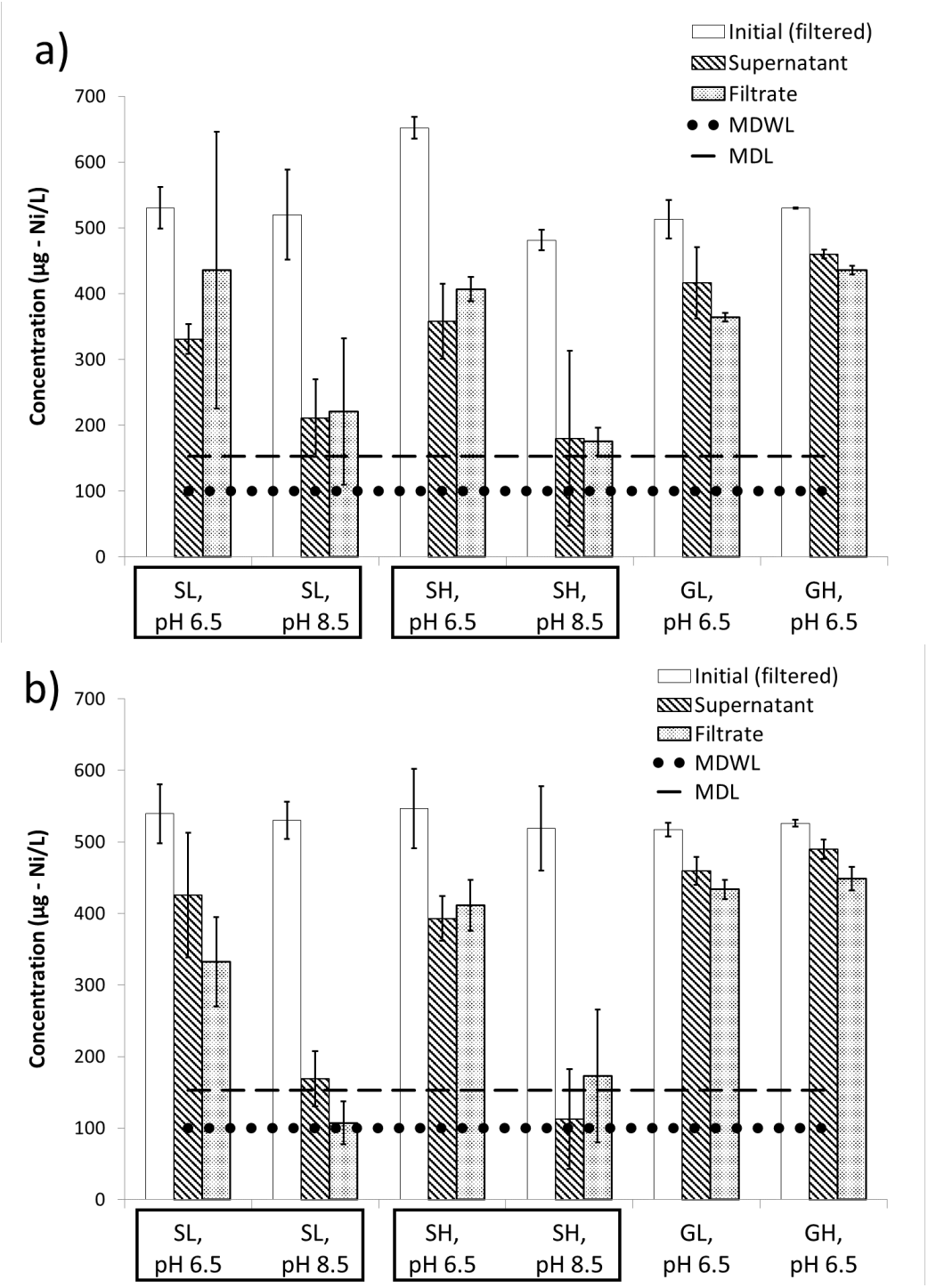

Figure 3.10: Nickel removal by a.) aluminum, and b.) iron electrocoagulation in six synthetic water matrices spiked with mixed contaminants. Test water types were abbreviated as follows: SL ("surface low"), SH ("surface high"), GL ("ground low"), GH ("ground high"). See Section 2.2 for a description of the four test water types. Values shown are means of triplicate tests; error bars are ±1 standard deviation.

next analyzed by Kruskal-Wallis ANOVA. The Kruskal-Wallis analysis showed a significant difference between the combinations ($X^2(3, 43) = 33.5$, $p < 0.0001$). A post hoc Bonferroni multiple comparison showed significant differences in nickel removal at pH 6.5 and pH 8.5 for both aluminum and iron electrodes. Aluminum and iron electrodes did not differ significantly at a given pH, though iron electrodes at pH 6.5 differed significantly from aluminum electrodes at pH 8.5. For both electrodes, removal was signficantly greater at pH 8.5 than pH 6.5, as shown in Table 3.3, page 53. The point estimates of mean removal also suggest the pH x electrode material interaction may be valid, with iron outperforming aluminum at pH 8.5 and aluminum outperforming iron at pH 6.5.

Aqueous $NiCO_3$ comprises approximately 1.5% of soluble nickel (II) at pH 6.5 in high alkalinity waters, as shown in Figure A.6, page 87. Postitive Ni^{2+} ions attracted to the cathode would experience more basic conditions. As shown in Figure A.6, $NiCO_{3(aq)}$ continues to increase in concentration until pH 9.5, where nickel (II) carbonate accounts for approximately 85% of soluble nickel (II). In surface waters, however, Ni^{2+} ions account for nearly all soluble nickel (II) in the pH range tested, as shown in Figure A.8, page 88. Because $NiCO_3$ is uncharged, adsorption to flocs was expected to be lower at higher pH. However, $NiCO_3$ may be more likely to form precipitates or a scale layer in the basic environment of the cathode.

In groundwaters, Box-Cox transformations of nickel removal showed significant effects for post-treatment ($F(1, 20) = 11.75$, $p = 0.0027$), test water ($F(1, 20) = 4.58$, $p = 0.045$), and electrode material ($F(1, 20) = 9.48$, $p = 0.0059$). Ground waters were tested only at pH 6.5. Nickel removal in groundwater was significantly higher after microfiltration ($M = 19.4\%$, $SD = 6.44\%$) than settling alone ($M = 12.4\%$, $SD = 7.30\%$). Aluminum electrodes ($M = 19.6\%$, $SD = 8.49\%$) routinely outperformed iron electrodes ($M = 12.3\%$, $SD = 4.46\%$). Finally, removal was greater in "ground high" than "ground low" test waters. Removal in all four test waters is shown in Table 3.4, page 54. Lower removal with increasing solids supports the hypothesis that nickel removal was inhibited by formation of charge-neutral $NiCO_3$ in solution.

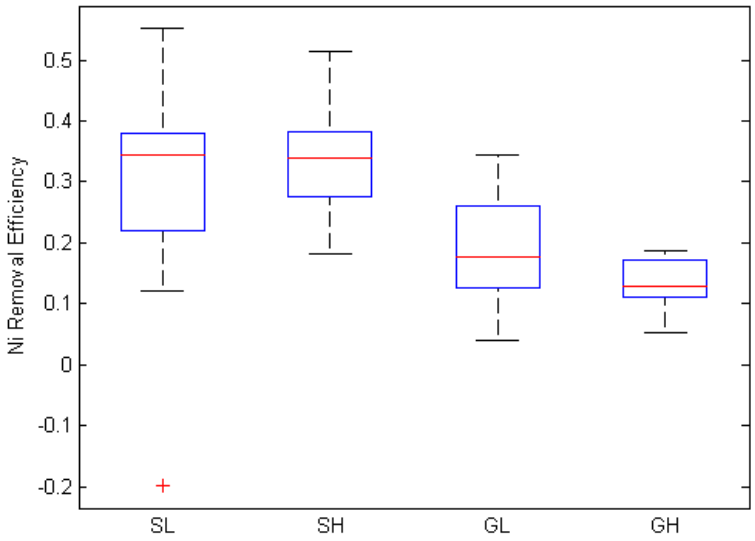

Figure 3.11: Nickel removal at pH 6.5 in the four synthetic test waters used in this study: "surface low" (SL), "surface high" (SH), "ground low" (GL), and "ground high". High-solids groundwaters show significantly less variation and poorer removal efficiencies than surface waters. Data are shown only for tests at pH 6.5 to accurately compare variance between test water types.

Table 3.3: Nickel removal efficiency, interaction between pH and electrode material. Aluminum outperformed iron electrodes at pH 6.5, while iron outperformed aluminum at pH 8.5. Values are for nickel removal from "surface low" and "surface high" test waters only.

		Electrode Material	
pH		Aluminum	Iron
6.5			
	n	12	12
	M	35%	28%
	SD	18%	11%
8.5			
	n	11	12
	M	61%	74%
	SD	16%	10%

Table 3.4: Nickel removal efficiency, summary matrix of test water and pH results. Removal efficiencies at pH 8.5 were greater than those at pH 6.5 for both surface waters. Nickel trended toward poorer removal with increasing ionic strength of the electrolyte, from "surface high" to "ground high".

		pH	
Test water		6.5	8.5
Surface Low			
	n	12	11
	M	29%	67%
	SD	19%	14%
Surface High			
	n	12	12
	M	34%	68%
	SD	10%	16%
Ground Low			
	n	12	0
	M	19%	NA *
	SD	9.2%	NA *
Ground High			
	n	12	0
	M	13%	NA *
	SD	4.5%	NA *

* Groundwaters were tested only at pH 6.5.

3.4.3 Arsenic

The results for arsenic removal in Phase 2 are shown in Figure 3.12, page 57. ANOVA analysis of arsenic removal efficiency under various test conditions showed potential effects from post-treatment, test water, and electrode material, as well as post-treatment x test water and post-treatment x electrode material interactions. However, grouping data by electrode type and post-treatment failed the assumptions of heteroscedacity and normality. Box-Cox transformations of the data were reanalyzed. Even after transformation, grouping data by significant variables continued to result in heteroscedastic and non-normal groups. In particular, the variation for settled samples using iron electrodes was too broad compared to settled samples for aluminum and filtered samples for either electrode material. Also, the tests using aluminum electrodes formed a non-normal distribution of results.

Transformed data were therefore analyzed separately by post-treatment (microfiltration versus settling only) with three-way ANOVA (pH, test water and electrode material). Analysis of filtered samples showed a strong effect from electrode material ($F(1, 30) = 848.4$, $p < 0.0001$). Analysis of settled samples showed effects from both electrode material ($F(1, 29) = 87.8$, $p < 0.0001$) and test water ($F(3, 29) = 3.22$, $p = 0.037$). In no analysis of the data was pH shown to have an effect.

As with chromium removal, iron electrodes ($M = 0.831$, $SD = 0.139$) drastically outperformed aluminum electrodes ($M = 0.173$, $SD = 0.174$). The superiority of iron electrodes was anticipated. Previous authors had proposed that ephemeral iron species oxidize arsenite to form arsenate, which is readily adsorbed to flocs (Li et al., 2012). Also like chromium, arsenic showed enhanced removal from microfiltration with iron electrodes but not with aluminum electrodes, as shown in Table 3.5, page 58. As previously mentioned, iron flocs were observed in suspension after centrifugation. The stochastic inclusion of these tiny flocs likely increased the overall arsenic concentration in digested samples. The lack of a significant difference between filtered and unfiltered samples after aluminum EC explains the interaction between electrode material and post-treatment.

Between test water types, arsenic removal followed the same trend seen in previous metals of decreasing performance with increasing TDS concentration: "surface low" ($M = 0.521$, $SD = 0.406$), "surface high" ($M = 0.578$, $SD = 0.373$), "ground low" ($M = 0.442$, $SD = 0.332$), "ground high" ($M = 0.403$, $SD = 0.307$). Though filtered samples did now show a significant effect from test water, point estimates (group means) show the same approximate trend, as shown in Table 3.6, page 58.

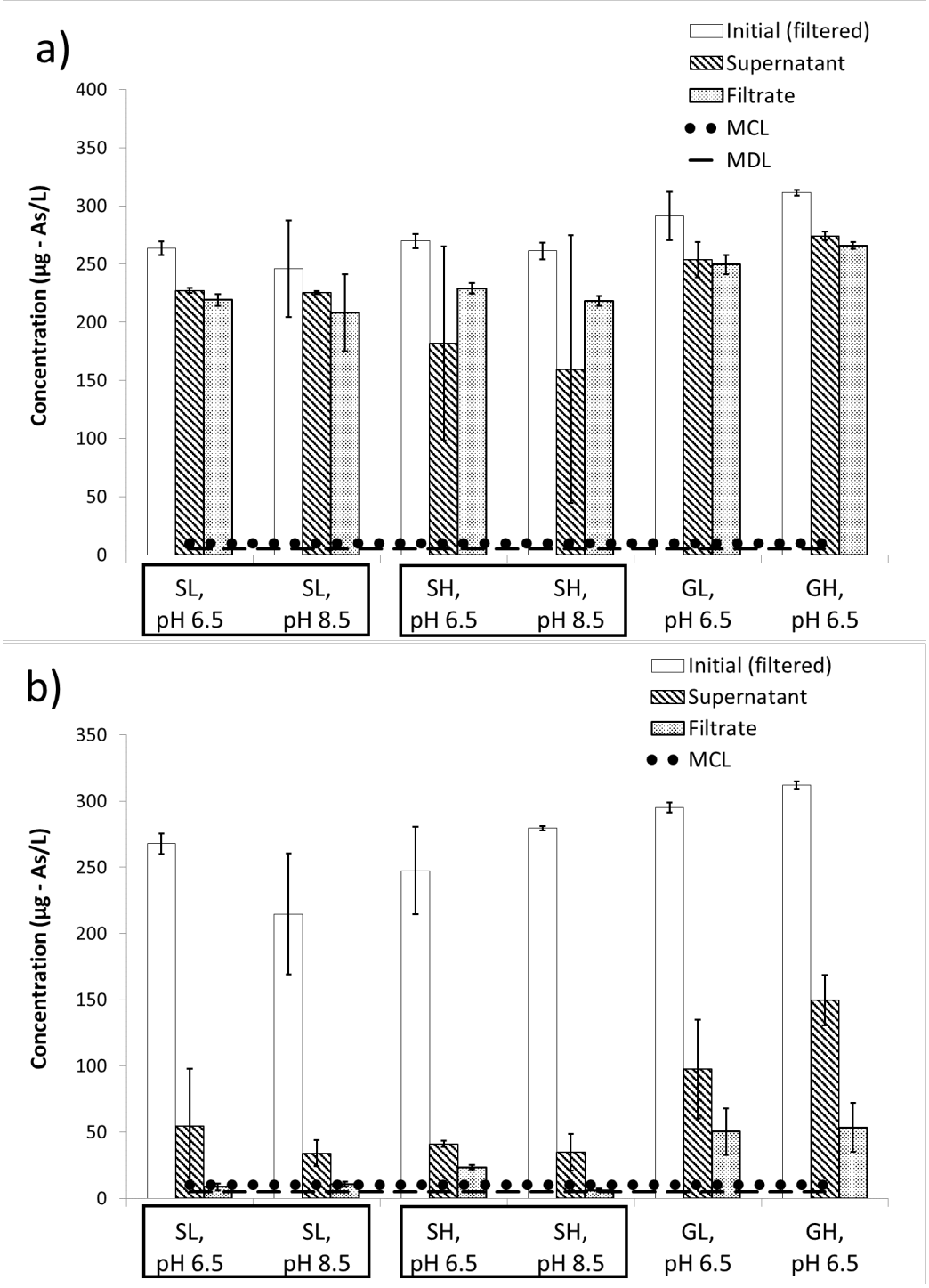

Figure 3.12: Arsenic removal by a.) aluminum, and b.) iron electrocoagulation in six synthetic water matrices spiked with mixed contaminants. Note the dramatic removal of arsenic with iron electrodes compared to that with aluminum electrodes. Test water types were abbreviated as follows: SL ("surface low"), SH ("surface high"), GL ("ground low"), GH ("ground high"). See Section 2.2 for a description of the four test water types. Values shown are means of triplicate tests; error bars are ±1 standard deviation.

Table 3.5: Arsenic removal efficiency, interaction between post-treatment and electrode material. Arsenic showed enhanced removal from microfiltration after EC with iron electrodes, but not aluminum electrodes.

		Electrode Material	
Post-treatment		Aluminum	Iron
Settling			
	n	17	18
	M	20%	76%
	SD	24%	15%
Microfiltration			
	n	18	18
	M	15%	91%
	SD	7.7%	7.0%

Table 3.6: Arsenic removal efficiency, interaction between test water and post-treatment. Values shown summarize data at pH 6.5 only to avoid confounding the effects of pH with those of test water type. Arsenic showed a trend of poorer removal with increasing ionic strength of the electrolyte, from "surface high" to "ground high," though this trend was significant only for unfiltered samples ("Settling").

		Post-treatment	
Test water		Settling	Microfiltration
Surface Low			
	n	6	6
	M	47%	57%
	SD	38%	44%
Surface High			
	n	6	6
	M	52%	53%
	SD	35%	41%
Ground Low			
	n	6	6
	M	40%	49%
	SD	31%	38%
Ground High			
	n	6	6
	M	32%	49%
	SD	22%	38%

3.4.4 Cadmium

The results for cadmium removal in Phase 2 are shown in Figure 3.13, page 60. Box-Cox transformations of the cadmium removal showed a significant interaction between pH and test water by ANOVA. Because not all test waters were tested at multiple pH levels, the data were further analyzed separately by both pH and surface versus ground water. In the four-way ANOVA of only synthetic "surface waters", pH ($F(1, 40) = 132.2$, $p < 0.0001$) and post-treatment ($F(1, 40) = 8.86$, $p = 0.0049$) effects were both significant variables. The test water x pH interaction remained significant when limited to results from the "surface" waters ($F(1, 40) = 4.87$, $p = 0.033$), along with an interaction between pH and electrode material ($F(1, 40) = 7.45$, $p = 0.0094$). In the three-way ANOVA of only synthetic "groundwaters", all three variables were very significant, with no significant interactions: post-treatment ($F(1, 20) = 27.96$, $p < 0.0001$), test water ($F(1, 20) = 74.19$, $p < 0.0001$), and electrode material ($F(1, 20) = 214.24$, $p < 0.0001$).

At pH 6.5, post-treatment ($F(1, 39) = 30.14$, $p < 0.0001$), test water ($F(3, 39) = 22.3$, $p < 0.0001$), and electrode material ($F(1, 39) = 114.9$, $p < 0.0001$) were all significant, with a significant interaction between test water and electrode material ($F(3, 39) = 18.07$, $p < 0.0001$). While the transformed data did not meet the assumption of homoscedacity when grouped by water type, grouping by combinations of electrode and water type resulted in homogeneous variance. At pH 8.5, only post-treatment was significant ($F(1, 19) =$, $p = 0.0056$), while electrode material was only significant for an α value of 0.1 ($F(1, 19) =$, $p = 0.086$).

Because cadmium was spiked at a low initial concentration (30 μg/L), the mean removal at pH 8.5 (86.0%) resulted in very low post-treatment concentrations (<5 μg/L Cd). Since the MDL for cadmium is 2.83 μg/L, removal efficiencies were most likely compressed beyond approximately 91.6% removal. In addition, cadmium is theoretically about 35% as soluble at pH 8.5 as it is at pH 6.5, as shown in Figure A.13, page 91. At pH 8.5, cadmium solubility was modeled to be approximately 10 μg/L assuming the potential to form all precipitates within the duration of the experiment. Microfiltered,

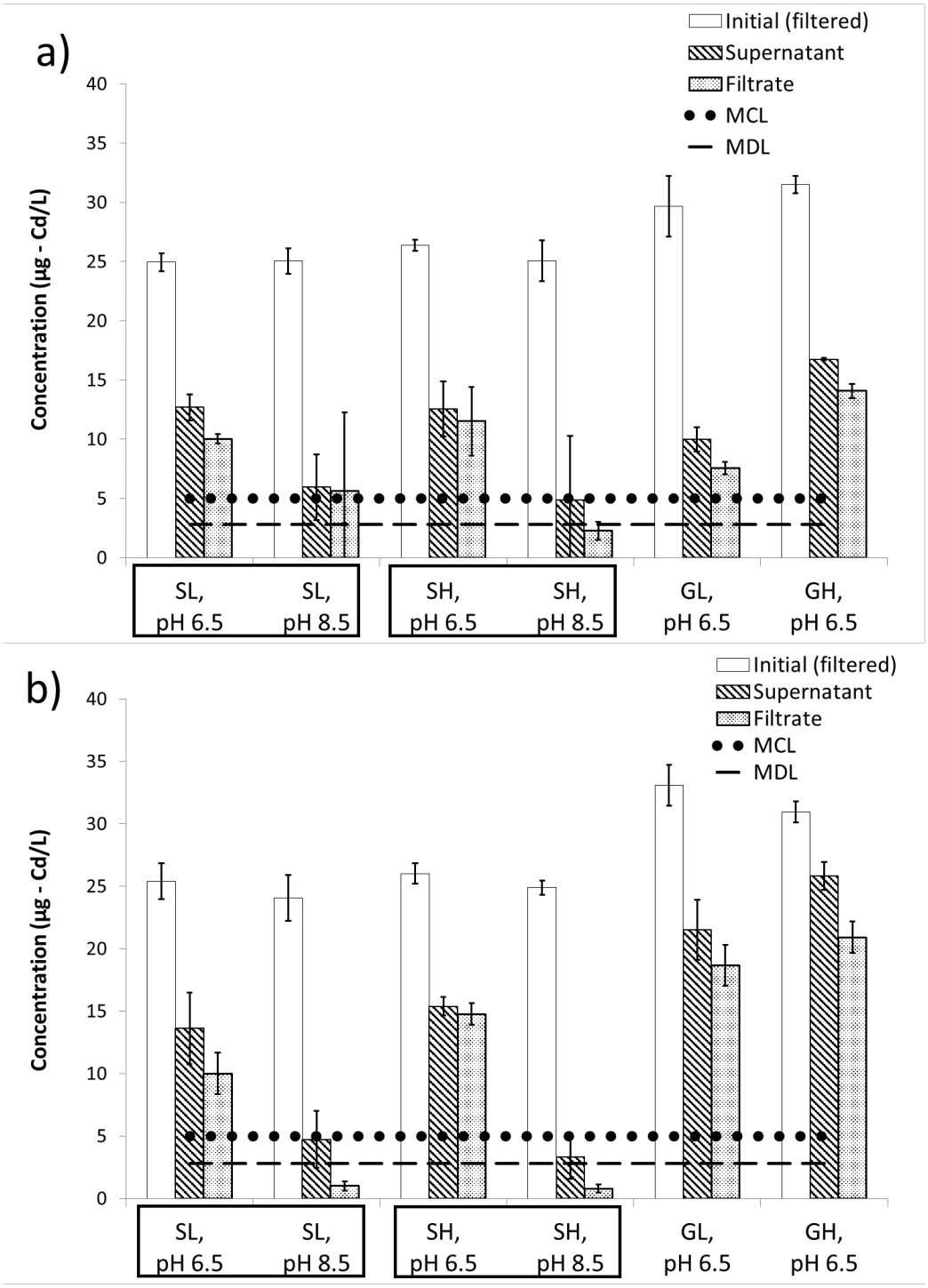

Figure 3.13: Cadmium removal by a.) aluminum, and b.) iron electrocoagulation in six synthetic water matrices spiked with mixed contaminants. Test water types were abbreviated as follows: SL ("surface low"), SH ("surface high"), GL ("ground low"), GH ("ground high"). See Section 2.2 for a description of the four test water types. Values shown are means of triplicate tests; error bars are ±1 standard deviation.

untreated samples show that soluble concentrations of approximately 30 μg/L were achieved even at pH 8.5. However, cadmium may have formed colloidal precipitates that were able to pass through a 0.45 μm filter. Such precipitates would have a higher density and lower charge density than truly aqueous species and would therefore be more readily destabilized. Cadmium removal may have been driven primarily by solubility, and the effect of other test variables would then be muted. Therefore, the significance of test water at pH 6.5 only (*i.e.*, the interaction between pH and test water) was likely an artifact of experimental design and not necessarily descriptive of actual EC performance.

At pH 6.5, aluminum electrodes outperformed iron electrodes, as shown in Table 3.7, page 62. However, the increase in performance was apparent only in ground waters, as shown in Figure 3.14, page 62. At pH 8.5, the mean removal for iron electrodes was slightly greater than that of aluminum electrodes. However, the three-way test at pH 8.5 found only a potentially significant ($\alpha = 0.1$) effect ($p = 0.086$) due to electrode material. In all cases, the mean removal efficiency was greater after filtration ($M = 0.656$, $SD = 0.221$) than settling alone ($M = 0.557$, $SD = 0.223$).

Comparison of removal in the four synthetic test waters shows an overall trend of decreasing removal with increasing TDS, particularly in the highest-solids water ("ground high"), as shown in Table 3.8, page 63. This trend was particularly apparent in tests using iron electrodes, as shown in Figure 3.15, page 62. Regardless of the pH x test water interaction, removal at pH 8.5 was consistently greater than that at pH 6.5, as shown in Table 3.9, page 64. As mentioned, the slight difference in removal between "surface low" and "surface high" at pH 8.5 was not significant.

Table 3.7: Cadmium removal efficiency, interaction between pH and electrode material. Aluminum electrodes outperformed iron electrodes at pH 6.5 only. At pH 8.5, mean cadmium removal with iron electrodes is higher than that with aluminum electrodes, but this difference was not found to be significant. Values are shown for "surface high" and "surface low" test waters only.

		Electrode Material	
pH		Aluminum	Iron
6.5			
	n	12	12
	M	54%	48%
	SD	7.6%	9.2%
8.5			
	n	11	12
	M	82%	90%
	SD	17%	9.2%

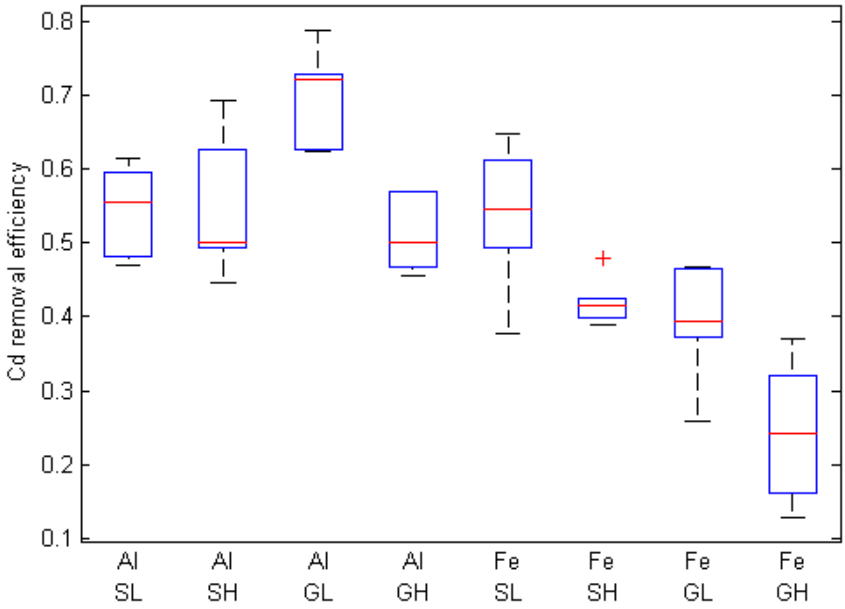

Figure 3.14: Cadmium removal efficiency by electrocoagulation with aluminum and iron electrodes in four synthetic water matrices (t = 2 min, I = 0.5 A). Aluminum electrodes out-performed iron electrodes in "ground low" and " ground high" waters. Iron electrodes showed poorer performance with the increase in electrolyte strength from "surface low" to "ground high." Data are shown only for tests at pH 6.5 to accurately compare variance between test water types.

Table 3.8: Cadmium removal efficiency, interaction between test water and electrode material. EC with iron electrodes showed decreasing cadmium removal efficiency with increasing ionic strength of the electrolyte from "surface low" to "surface high." EC with aluminum electrodes did not show this trend. Values are shown for pH 6.5 only to avoid confounding the effect of pH with that of water type.

		Electrode Material	
Test water		Aluminum	Iron
Surface Low			
	n	6	6
	M	55%	54%
	SD	6.2%	9.6%
Surface High			
	n	6	6
	M	54%	42%
	SD	9.5%	3.2%
Ground Low			
	n	6	6
	M	70%	39%
	SD	6.4%	7.6%
Ground High			
	n	6	6
	M	51%	24%
	SD	5.1%	9.5%

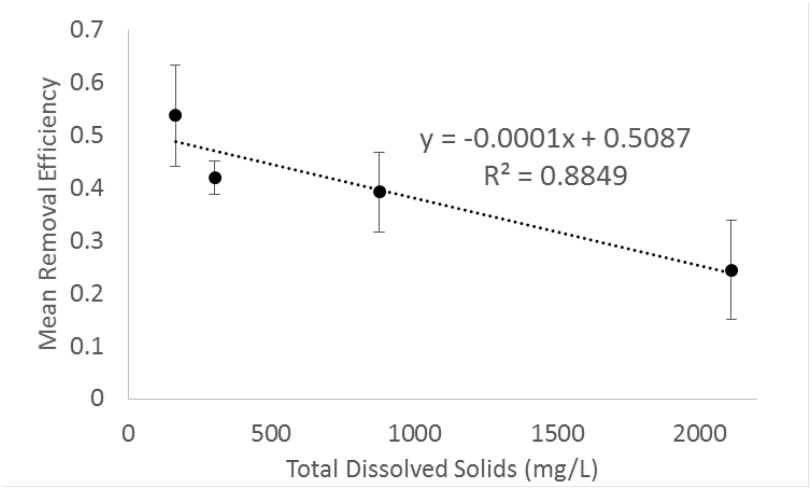

Figure 3.15: Effect of TDS on cadmium removal efficiency by electrocoagulation with iron electrodes (t = 2 min, I = 0.5 A). Data are shown only for tests at pH 6.5. Error bars represent one standard deviation.

Table 3.9: Cadmium removal efficiency, interaction between pH and test water. "Ground high" water showed significantly lower removal than the other three water types at pH 6.5. At pH 8.5, the slight increase in mean cadmium removal from "surface low" to "surface high" was not significant.

		pH	
Test water		6.5	8.5
Surface Low			
	n	12	11
	M	54%	83%
	SD	7.7%	16%
Surface High			
	n	12	12
	M	48%	89%
	SD	9.3%	12%
Ground Low			
	n	12	0
	M	55%	NA *
	SD	18%	NA *
Ground High			
	n	12	0
	M	38%	NA *
	SD	16%	NA *

* Groundwaters were tested only at pH 6.5.

3.4.5 Lead

The results for lead removal in Phase 2 are shown in Figure 3.16, page 66. Lead removal showed significant effects from post-treatment and pH. However, grouping data by either variable showed that the resulting groups were heteroscedastic. Box-Cox transformation of the data resolved for homogeneous variance and normality, but also revealed a likely interaction between pH and test water. Data were divided by pH and analyzed by three-way ANOVA (post-treatment, test water, electrode material), then by surface water versus groundwater and analyzed by a four-way (post-treatment, pH, test water, electrode material) and a three-way ANOVA test (post-treatment, test water, electrode material), respectively. This approach allowed separation of pH effects from test water effects.

At pH 6.5, transformed data showed significant effects from post-treatment ($F(1, 39) = 154.5$, $p < 0.0001$), test water ($F(3, 39) = 3.95$, $p = 0.015$), and electrode material ($F(1, 39) = 9.24$, $p = 0.0042$). Post-treatment and test water also showed a significant interaction ($F(3, 39) = 3.04$, $p = 0.040$). At pH 8.5, transformed data showed a potentially significant effect only from post-treatment ($F(1, 19) = 3.24$, $p = 0.088$).

Analysis of surface water data showed only an effect from post-treatment ($F(1, 41) = 21.61$, $p < 0.0001$) and a potentially significant interaction between post-treatment and test water ($F(1, 41) = 3.93$, $p = 0.054$). Analysis of groundwater data indicated possible effects from post-treatment, as well as two- and three-way interactions between test water, electrode material and post-treatment. However, data were heteroscedastic in all combinations, including between triplicate results for individual test conditions. Therefore, the assumptions for ANOVA were not met. Furthermore, the potential three-way interaction between all independent variables indicates the absence of any prevailing pattern in test treatments in groundwater tests.

Though electrode material was shown to be have a significant effect on lead removal at pH 6.5, the magnitude of the difference between removal at pH 6.5 with iron electrodes ($M = 0.888$, $SD = 0.0926$) and aluminum electrodes ($M = 0.876$, $SD = 0.0623$)

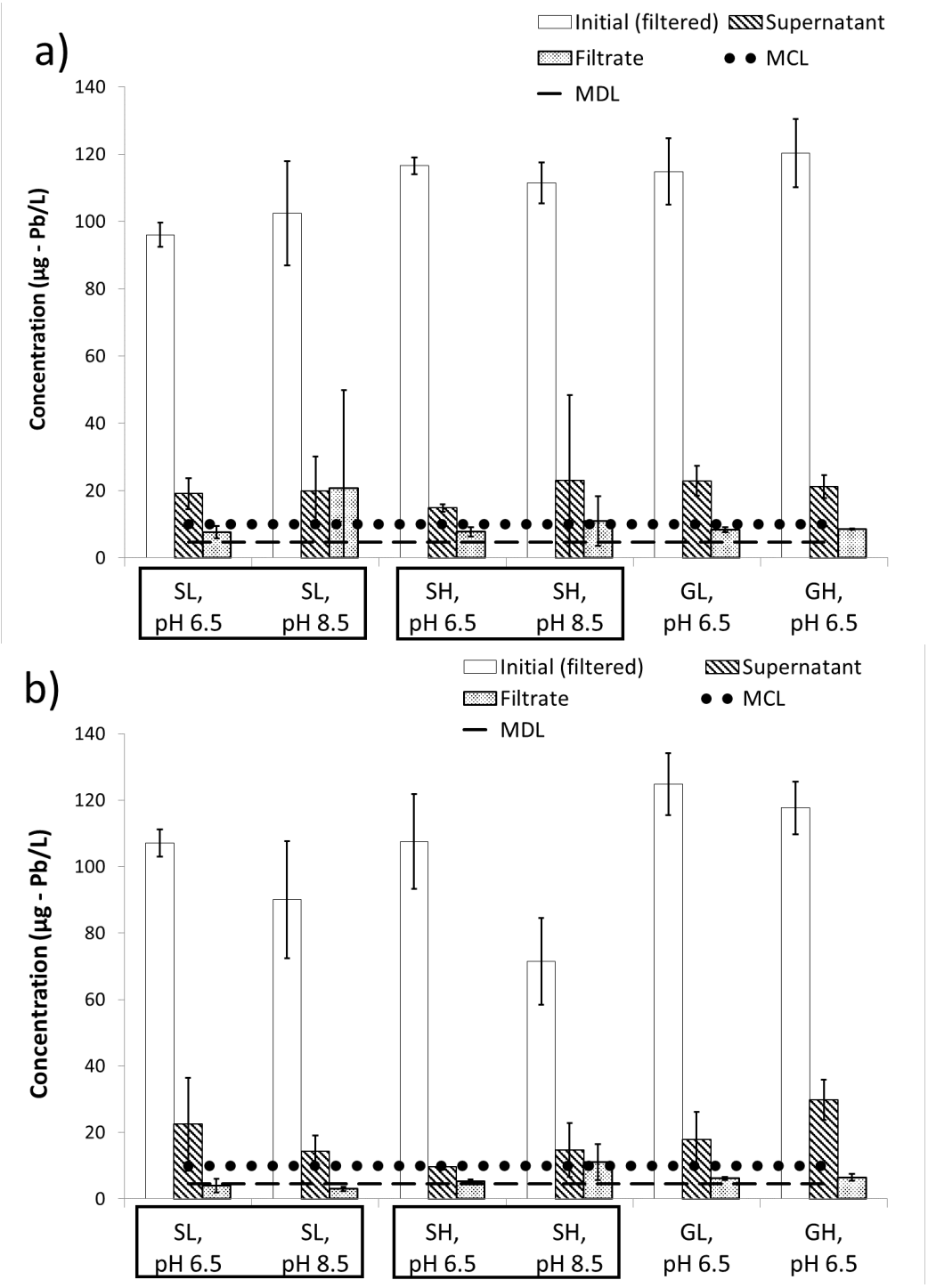

Figure 3.16: Lead removal by a.) aluminum, and b.) iron electrocoagulation in six synthetic water matrices spiked with mixed contaminants. Test water types were abbreviated as follows: SL ("surface low"), SH ("surface high"), GL ("ground low"), GH ("ground high"). See Section 2.2 for a description of the four test water types. Values shown are means of triplicate tests; error bars are ±1 standard deviation.

was not great enough to be meaningful in application. Microfiltration enhanced lead removal, as shown in Table 3.10, page 68. While post-treatment was only significant for an α value of 0.1 ($p = 0.088$) at pH 8.5, Table 3.10 shows the same trend holds for the point estimates (group means) of lead removal.

As observed for previous metals, lead removal efficiency decreased in high-solids waters. However, the trend was not apparent in filtered samples, which uniformly showed greater than 90% removal, as shown in Table 3.11, page 68. Though pH was initially suspected to be significant, further analysis of surface waters alone (the only waters tested at multiple pH levels) revealed pH to be insignificant ($F(1, 41) = 2.68$, $p = 0.11$).

Table 3.10: Lead removal efficiency, summary matrix of pH and post-treatment results. Mean removal was greater after microfiltration than settling alone, though this effect was only significant at pH 6.5. Values at pH 6.5 summarize tests in "surface high" and "surface low" test waters only to avoid confounding the effect of pH with that of water type.

		Post-treatment	
pH		Settling	Microfiltration
6.5			
	n	12	12
	M	84%	94%
	SD	8.1%	2.2%
8.5			
	n	11	12
	M	80%	88%
	SD	13%	14%

Table 3.11: Lead removal efficiency, interaction between test water and post-treatment. Settled samples show a trend of decreasing lead removal with increasing ionic strength of the electrolyte from "surface low" to "ground high". Microfiltered samples show no such trend, possibly due to consistently excellent removal. Values shown summarize tests at pH 6.5 only to avoid confounding the effect of pH with that of test water type.

		Post-treatment	
Test water		Settling	Microfiltration
Surface Low			
	n	6	6
	M	79%	94%
	SD	9.2%	3.0%
Surface High			
	n	6	6
	M	89%	94%
	SD	2.4%	1.2%
Ground Low			
	n	6	6
	M	83%	94%
	SD	6.4%	1.4%
Ground High			
	n	6	6
	M	79%	94%
	SD	5.4%	1.0%

3.5. Objective 2: Reactor parameters

3.5.1 Electrode material

Aluminum and iron electrodes starkly contrasted in removal of chromium and arsenic, with poor removal from aluminum electrodes and greater than 90% removal from iron. Iron's superior performance came despite a molar loading rate nearly three times lower than that of aluminum. In the two-minute tests with mixed contaminants, reduction to below the MCL for these metals was achieved only with iron electrodes. Nickel, cadmium and lead removal at pH 6.5 was greater with aluminum than iron electrodes. Aluminum electrodes were expected to provide better cation removal at pH 6.5 because of the negative charge of aluminum hydroxides above approximately pH 6 (see Figure A.1, page 84), whereas iron (III) hydroxides have a positive charge below pH 9 (see Figure A.2, page 85). In addition, aluminum is minimally soluble slightly above pH 6. However, both nickel and cadmium showed no significant difference between electrodes at pH 8.5, with a slightly greater mean removal by iron electrodes. Removal was also greater for both metals at pH 8.5 than at pH 6.5. More importantly, aluminum only had a slight edge over iron, even where that edge was statistically significant. To meet secondary standards for aluminum and iron, aluminum is preferable at pH 6.5, and iron is preferable at pH 8.5. In light of aluminum's potential neurotoxicity, however, iron may be preferable for most applications.

3.5.2 Post-treatment

Post-treatment with microfiltration increased removal of all metals, though significance was often demonstrated only for a subset of tests. For chromium and arsenic, microfiltration enhanced contaminant removal for iron electrodes but not aluminum electrodes. This trend supports observations during the tests. Iron coagulants formed small, slowly-settling flocs, while aluminum coagulants formed large, macro-flocs that readily settled or floated to the surface. Thus, iron flocs were expected to require filtration

beyond gravitational separation. The high variation in supernatant samples likely arose from stochastic inclusion of small flocs. Settled samples were subjected to relatively weak centrifugation before decanting, and the chance inclusion of small flocs in the sample could greatly influence the contaminant concentration. This variance in settled iron samples is likely indicative of real-world conditions and not an artifact of experimental design. Even where microfiltration did not reduce the mean removal efficiency, microfiltration reduced the variation in samples. Thus, microfiltration should be considered a valuable post-treatment for EC, especially in reactors with iron electrodes.

3.6. Objective 3: Water quality parameters

3.6.1 pH

Cadmium and nickel both exhibited enhanced removal at pH 8.5 compared to pH 6.5, while the remaining metals showed no significant difference in removal over the range tested. While cadmium was expected to be less soluble at pH 8.5 based on equilibrium modeling, nickel was expected to be soluble at the spiked level to at least pH 9 (see Figure A.7). Aluminum as well as iron electrodes were shown to be more effective at pH 8.5 for cadmium and nickel, so decreased coagulant solubility is an unlikely cause for greater removal. Speciation is also unlikely to have resulted in greater removal, as Cd^{2+} and Ni^{2+} remain the dominant species between pH 6.5 and 8.5. Close to pH 8.5, the uncharged, aqueous species $CdCO_3$ and $NiCO_3$ begin to account for a relevant fraction of dissolved species (see Figures A.13, page 91, and A.6, page 87). Of the remaining three metals tested, lead shares a similar speciation scheme, with the exception that $PbHCO_3^+$ may be dominant over Pb^{2+} at pH 6.5 with a sufficient concentration of bicarbonate (see Figures A.14, page 91, and A.16, page 92). However, pH was not a significant variable for lead. In fact, mean lead removal was slightly greater at pH 6.5 than pH 8.5 (see Table 3.10, page 68).

The uncharged carbonate species were expected to be less likely to co-precipitate in flocs, not more likely. Given the negative charge of aluminum hydroxides above pH 6

and positive charge of iron hydroxides below pH 8.5, differential removal was expected between electrodes if the primary mechanism of removal was adsorption or co-precipitation. However, if the primary mechanism of removal at pH 8.5 was enmeshment (sweep flocculation), carbonate species' lack of charge may allow better agglomeration. Previous experiments have shown precipitation of calcium and magnesium carbonate onto the cathode (Malakootian et al., 2010; Vik et al., 1984). Reversing the polarity of the electrodes was expected to re-dissolve scale or prevent its formation, but this effect was not demonstrated. In addition, given the pH and concentration gradients present in an EC reactor, speciation and solubility are likely more complex than can be represented by an equilibrium model.

3.6.2 Water matrix composition

All metals showed decreasing removal efficiency with an increase in the ionic strength of the test water. For arsenic and lead removal, the subset of microfiltered samples did not show the same trend due to the water matrix, likely because overall variation between filtered concentrations was low due to very high removal. Differences between synthetic waters cannot be attributed to any one species or even broad water quality parameters like hardness, alkalinity or ionic strength. The objective of this study was not to delineate the fundamental water chemistry of EC, but rather to evaluate performance across a representative range of water matrices. Nonetheless, the trend was uniform across metals with disparate speciation schemes. In particular, arsenic and chromium were not expected to show any speciation with the background electrolytes in either stable valence state (see Figures A.11 - A.5, pages 90 - 86). In addition, destabilization of charged particles from electrical double layer compression should increase with the ionic strength of the solution. Therefore, the decreased removal efficiency with high ionic strength is likely due to change(s) in the flocs themselves.

Bicarbonate, calcium and magnesium were expected to encourage the formation of denser, more crystalline flocs in iron (van Genuchten et al., 2014). By observation, aluminum flocs in high-solids waters also formed a more dense pellet after centrifugation

and took on a dull, gray hue compared to the loose, whitish-gray pellet observed in surface water tests. The background electrolytes likely adsorbed to or co-precipitated in the flocs, thereby competing for sorption sites and reducing the floc surface charge.

3.6.3 Power consumption

As expected, power consumption decreased with increases in TDS concentration. Table 3.12 on page 73 shows the mean conductivity and applied voltage for each test water. The resistance of each test water was also calculated by Equation 1.4, page 13, where the cell constant was estimated by the interelectrode distance and face area of the plate electrodes ($\frac{l}{A} = \frac{1cm}{54cm^2}$). The theoretical IR drop was calculated from this resistance according to Ohm's law, Equation 1.5, page 13. Power was calculated by the actual, measured applied potential according to Equation 2.1, page 27. Applied energy was calculated as the product of the power and the treatment time (2 minutes), normalized by the volume of the reactor (300 mL). Aluminum and iron electrodes showed no significant difference in applied potential.

Table 3.12 shows that the theoretical potentials required to overcome the IR drop in each test water closely match the actual applied potentials. Thus, power can be assumed to be primarily a function of the IR drop. This relationship is shown in Figure 3.17, page 73, in which power increases linearly with the inverse of conductivity (*i.e.*, resistivity). Due to the low conductivity of potable water, the IR drop demands a much higher applied potential than kinetic or mass transfer overpotentials alone. The reactor used in this study was by no means optimized for energy efficiency. A smaller interelectrode distance and larger ratio of electrode surface area to reactor volume (*e.g.,* by increasing the number of electrodes) would lower the energy demand of the reactor.

Table 3.12: Conductivity, potential and power consumption in four test waters. Note that in some cases the actual applied voltage was slightly less than the theoretical potential required by the IR drop. This discrepancy indicates a small error in the cell constant, which was estimated from electrode dimensions. Applied energy was calculated based on two minutes of treatment.

	Conductivity	Resistance	Potential (V)		Applied Energy
	(mS/cm)	(ohm)	IR Drop	Applied Potential	(MJ/m^3)
Surface low					
mean	0.26	72	36	32	6.4
s	0.018			1.9	
n	24			24	
Surface high					
mean	0.47	40	20	19	3.7
s	0.013			0.82	
n	24			24	
Ground low					
mean	1.3	15	7.3	7.9	1.6
s	0.011			0.35	
n	12			12	
Ground high					
mean	3.1	6.0	3.0	4.9	0.84
s	0.15			0.15	
n	12			12	

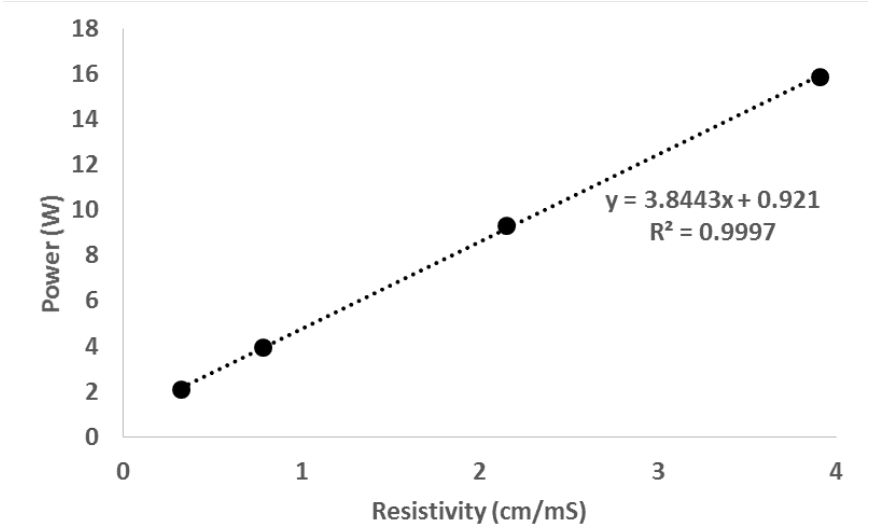

Figure 3.17: Reactor power consumption as a function of resistivity.

4. CONCLUSIONS

Removal to below drinking water standards was demonstrated for five of seven metal contaminants: chromium, copper, arsenic, cadmium and lead. Removal of these metals to below drinking water standards was also demonstrated in a mixed-contaminant scenario, with the exception of copper, which was not tested with other contaminants. EC apparently removed zinc to below the secondary standard of 5 mg/L. However, the method detection limit for zinc was higher than the standard, so the post-treatment concentrations cannot be confirmed. Nickel was not removed to below the secondary standard, though removal to near the limit was shown after two minutes of treatment at pH 8.5. Zinc and nickel contamination posed a significant challenge in the first phase of testing (single contaminants). Due to the high concentration of aluminum and iron after running the reactor for 15 minutes, samples required 100x dilution before they could be analyzed. The high dilution dramatically exaggerated the influence of ultra-low levels of contaminants in the diluent acid. Later tests of nickel removal in a mixed-contaminant solution with a 2 minute retention time required only a 10x dilution. These tests had a much lower detection limit for all contaminants, but nickel was not removed to below drinking water limits within the retention time.

As anticipated, iron electrodes showed far greater removal of chromium and arsenic than aluminum electrodes, most likely due to redox reactions between ferrous iron and the contaminants. Aluminum electrodes were only slightly more effective at removing nickel, cadmium and lead, and only at pH 6.5. Thus, the marked advantage of iron electrodes with arsenic and chromium outweighed the small advantage of aluminum electrodes with the remaining metals. Other factors not considered in this study, such as air sparging or the presence of NOM, may alter the relative effectiveness of aluminum or iron electrodes.

Microfiltration improved consistency and efficiency of removal of all metals, particularly for iron electrodes. In addition, microfiltration was required to significantly reduce residual aluminum and iron concentrations after treatment. Residual aluminum concentration was on average double the secondary drinking water standard, while iron

residuals were within 0.05 mg/L of the secondary standard. At pH 6.5, aluminum concentrations met the secondary standard of 0.20 mg/L, but not the lower range of 0.05 mg/L (US EPA, 2009). At pH 8.5, iron concentrations met the secondary standard of 0.3 mg/L. Despite the slight excess of iron at low pH levels, removal of contaminant metals to safe levels should outweigh non-enforceable, aesthetic limits. However, considering the potential neurotoxicity of aluminum, the Hippocratic principle, "Do no harm," prevails, and aluminum electrodes should not be used in high or variable pH waters.

The initial pH of the source water was not a significant factor for chromium, arsenic or lead. Nickel and cadmium showed markedly greater removal at pH 8.5 than pH 6.5. The reason for lower removal is uncertain, but both metals form carbonate species in the pH range tested. Nickel or cadmium carbonate may have precipitated onto the cathode surface, as has been observed for calcium carbonate. Alternatively, the lack of charge on the carbonate species may have allowed for more effective destabilization. Cadmium in particular may have also more readily precipitated at higher pH due to lower solubility. However, the low solubility was not reflected in cadmium concentrations in untreated, microfiltered samples.

All metals exhibited poorer removal efficiencies as the ionic strength of the water increased, particularly in the very high-solids, synthetic groundwaters. Hardness, alkalinity, sulfate and chloride concentrations all increased from surface waters to groundwaters. Nevertheless, the uniform affect on all contaminants suggests that decreased efficiency is due to alteration of aluminum and iron flocs. The background electrolytes most likely competed with contaminants by co-precipitating in, or adsorbing to, the flocs. The change in ionic strength between test waters also affected the applied potential on the cell.

Unfortunately, any change in an initial reactor or water quality parameter implies a change in numerous other parameters. For instance, holding coagulant dose, CLR and potential constant would require integrating the charge from varying current to establish the correct residence time. Thus, the current density and residence time would still change between tests. Even a difference in the effective electrode area in the reactor would change the reactor hydraulics and the dipole field driving electrophoresis. Likewise, the mass and

molar concentrations of aluminum and iron ions in solution necessarily differed with the same CLR because of their different valences and molecular weights. In this study, CLR and treatment time were deemed most fundamental, because coagulant dose is directly related to current and time but only indirectly related to voltage. A full-scale electrocoagulation reactor would likely control these two operating parameters (*e.g.*, rather than applied potential or anode surface area), regardless of the source water or electrode material.

This research demonstrated the effectiveness of EC in removing trace heavy metals for drinking water applications. In addition, the study provided an extensive analysis showing the relative importance of electrode material, post-treatment, and source water characteristics. Wherever possible, iron should be sought as an alternative to aluminum electrodes for reasons of both effectiveness and the safety of residuals for human consumption. Post-treatment filtration is highly recommended for contaminant polishing and limiting coagulant residuals. However, the optimal pore size and filter design remains to be determined. The wide range of test waters in this study demonstrated that the increase in power due to ohmic dissipation is at least partially balanced by greater removal in low ionic strength waters. In addition, water with higher ionic strength will require longer treatment times to achieve similar removal efficiency. Further testing is required to determine an optimal range of contaminant removal versus power demand.

BIBLIOGRAPHY

Abdel-gawad, S. A., Baraka, A. M., Omran, K. A., & Mokhtar, M. M. (2012). Removal of Some Pesticides from the Simulated Waste Water by Electrocoagulation Method Using Iron Electrodes . *Int. J. Electrochem. Sci.*, *7*, 6654–6665.

Akbal, F., & Camcı, S. (2012). Treatment of Metal Plating Wastewater by Electrocoagulation. *Environmental Progress & Sustainable Energy*, *31*, 340–350.

American Public Health Association, American Water Works Association, & Water Environment Federation (1998). *Standard Methods for the Examination of Water and Wastewater*. Washington, DC.: American Public Health Association, 20 ed.

Anawar, H. M., Akai, J., Mostofa, K. M. G., Safiullah, S., & Tareq, S. M. (2002). Arsenic poisoning in groundwater: Health risk and geochemical sources in Bangladesh. *Environment International*, *27*, 597–604.

Arroyo, M. G., Pérez-Herranz, V., Montañés, M. T., García-Antón, J., & Guiñón, J. L. (2009). Effect of pH and chloride concentration on the removal of hexavalent chromium in a batch electrocoagulation reactor. *Journal of Hazardous Materials*, *169*(1-3), 1127–33.

Bagga, A., Chellam, S., & Clifford, D. (2008). Evaluation of iron chemical coagulation and electrocoagulation pretreatment for surface water microfiltration. *Journal of Membrane Science*, *309*, 82 – 93.

Behloul, M., Grib, H., Drouiche, N., Abdi, N., Lounici, H., & Mameri, N. (2013). Removal of malathion pesticide from polluted solutions by electrocoagulation: Modeling of experimental results using response surface methodology. *Separation Science and Technology*, *48*(4), 664–672.

Ben-Sasson, M., Lin, Y., & Adin, a. (2011). Electrocoagulation-membrane filtration hybrid system for colloidal fouling mitigation of secondary-effluent. *Separation and Purification Technology*, *82*, 63–70.

Ben-Sasson, M., Zidon, Y., Calvo, R., & Adin, A. (2013). Enhanced removal of natural organic matter by hybrid process of electrocoagulation and dead-end microfiltration. *Chemical Engineering Journal*, *232*, 338–345.

Bhatnagar, R., Joshi, H., Mall, I. D., & Srivastava, V. C. (2014). Electrochemical treatment of acrylic dye-bearing textile wastewater: optimization of operating parameters. *Desalination and Water Treatment*, *52*(1-3), 111–122.

Cantor, K. P. (1997). Drinking Water and Cancer. *Cancer Causes & Control*, *8*(3), 292 – 308.

Cataldo Hernández, M., Barletta, L., Dogliotti, M. B., Russo, N., Fino, D., & Spinelli, P. (2012). Heavy metal removal by means of electrocoagulation using aluminum electrodes for drinking water purification. *Journal of Applied Electrochemistry*, *42*(9), 809–817.

Chen, X., Chen, G., & Yue, P. L. (2000). Separation of pollutants from restaurant wastewater by electrocoagulation. *Separation and Purification Technology*, *19*(1–2), 65 – 76.

Cheung, K. C., Poon, B. H. T., Lan, C. Y., & Wong, M. H. (2003). Assessment of metal and nutrient concentrations in river water and sediment collected from the cities in the Pearl River Delta, South China. *Chemosphere*, *52*(9), 1431–40.

Crittenden, J., Rhodes Trussel, R., Hand, D., Howe, K., & Tchobanoglous, G. (2013). *MWH's Water Treatment Principles and Design*. Hoboken: John Wiley & Sons, 3 ed.

Daous, M. A., & El-Shazly, A. H. (2012). Enhancing the Performance of a Batch Electrocoagulation Reactor for Chromium Reduction Using Gas Sparging. *Int. J. Electrochem. Sci.*, *7*, 3513–3526.

de Mello Ferreira, A., Marchesiello, M., & Thivel, P.-X. (2013). Removal of copper, zinc and nickel present in natural water containing Ca2+ and ions by electrocoagulation. *Separation and Purification Technology*, *107*, 109–117.

Den, W., & Wang, C.-J. (2008). Removal of silica from brackish water by electrocoagulation pretreatment to prevent fouling of reverse osmosis membranes. *Separation and Purification Technology*, *59*(3), 318–325.

Dermentzis, K., Christoforidis, A., & Valsamidou, E. (2011). Removal of nickel, copper, zinc and chromium from synthetic and industrial wastewater by electrocoagulation. *International Journal of Environmental Sciences*, *1*(5), 697–710.

Dubrawski, K. L., & Mohseni, M. (2013a). In-situ identification of iron electrocoagulation speciation and application for natural organic matter (NOM) removal. *Water Research*, *47*(14), 5371–5380.

Dubrawski, K. L., & Mohseni, M. (2013b). Standardizing electrocoagulation reactor design: iron electrodes for NOM removal. *Chemosphere*, *91*(1), 55–60.

Ellis, A. S., Johnson, T. M., & Bullen, T. D. (2002). Chromium isotopes and the fate of hexavalent chromium in the environment. *Science (New York, N.Y.)*, *295*(2002), 2060–2062.

Farhadi, S., Aminzadeh, B., Torabian, A., Khatibikamal, V., & Alizadeh Fard, M. (2012). Comparison of COD removal from pharmaceutical wastewater by electrocoagulation, photoelectrocoagulation, peroxi-electrocoagulation and peroxi-photoelectrocoagulation processes. *Journal of Hazardous Materials*, *219-220*(2012), 35–42.

Fernandes, A., Spranger, P., Fonseca, A., Pacheco, M., Ciríaco, L., & Lopes, A. (2014). Effect of electrochemical treatments on the biodegradability of sanitary landfill leachates. *Applied Catalysis B: Environmental*, *144*(0), 514 – 520.

Flaten, T. P. (2001). Aluminium as a risk factor in alzheimer's disease, with emphasis on drinking water. *Brain Research Bulletin*, *55*(2), 187 – 196. Metals and the Brain.

Gao, S., Du, M., Tian, J., Yang, J., Yang, J., Ma, F., & Nan, J. (2010). Effects of chloride ions on electro-coagulation-flotation process with aluminum electrodes for algae removal. *Journal of Hazardous Materials*, *182*(1-3), 827–34.

Garcia, N., Moreno, J., Cartmell, E., Rodriguez-Roda, I., & Judd, S. (2013). The cost and performance of an MF-RO/NF plant for trace metal removal. *Desalination*, *309*, 181–186.

García-Lara, a. M., Montero-Ocampo, C., & Martínez-Villafañe, F. (2009). An empirical model for treatment of arsenic contaminated underground water by electrocoagulation process employing a bipolar cell configuration with continuous flow. *Water science and technology : a journal of the International Association on Water Pollution Research*, *60*(8), 2153–2160.

Gomes, J., Daida, P., Kesmez, M., Weir, M., Moreno, H., Parga, J. R., Irwin, G., McWhinney, H., Grady, T., Peterson, E., & Cocke, D. L. (2007). Arsenic removal by electrocoagulation using combined Al-Fe electrode system and characterization of products. *Journal of Hazardous Materials*, *139*(2), 220–31.

Holt, P. K., Barton, G. W., & Mitchell, C. a. (2005). The future for electrocoagulation as a localised water treatment technology. *Chemosphere*, *59*(3), 355–67.

Jarup, L. (2003). Hazards of heavy metal contamination. *British Medical Bulletin*, *68*(1), 167–182.

Kuokkanen, V., Kuokkanen, T., Rämö, J., & Lassi, U. (2013). Recent Applications of Electrocoagulation in Treatment of Water and Wastewater—A Review. *Green and Sustainable Chemistry*, *03*(02), 89–121.

Li, J., Bai, J., Huang, K., Zhou, B., Wang, Y., & Hu, X. (2014). Removal of trivalent chromium in the complex state of trivalent chromium passivation wastewater. *Chemical Engineering Journal*, *236*, 59 – 65.

Li, L., van Genuchten, C. M., Addy, S. E. a., Yao, J., Gao, N., & Gadgil, A. J. (2012). Modeling As(III) oxidation and removal with iron electrocoagulation in groundwater. *Environmental Science & Technology*, *46*(21), 12038–45.

Lim, H.-S., Lee, J.-S., Chon, H.-T., & Sager, M. (2008). Heavy metal contamination and health risk assessment in the vicinity of the abandoned Songcheon Au–Ag mine in Korea. *Journal of Geochemical Exploration*, *96*(2-3), 223–230.

Liu, H., Zhao, X., & Qu, J. (2010). Electrocoagulation in water treatment. In C. Comninellis, & C. Guohua (Eds.) *Electrochemistry for the Environment*, (pp. 245 – 262). New York: Springer.

Malakootian, M., Mansoorian, H., & Moosazadeh, M. (2010). Performance evaluation of electrocoagulation process using iron-rod electrodes for removing hardness from drinking water. *Desalination*, *255*, 67–71.

Matsui, Y., Matsushita, T., Sakuma, S., Gojo, T., Mamiya, T., Suzuoki, H., & Inoue, T. (2003). Virus inactivation in aluminum and polyaluminum coagulation. *Environ. Sci. Technol.*, *37*, 5175 – 5180.

Meng, X., Korfiatis, G. P., Bang, S., & Bang, K. W. (2002). Combined effects of anions on arsenic removal by iron hydroxides. *Toxicology Letters*, *133*(1), 103 – 111.

Metcalf and Eddy, Tchobanoglous, G., Burton, F. L., & Stensel, H. D. (2003). *Wastewater Engineering: Treatment and Reuse*. Boston: McGraw Hill, 4 ed.

Moreno, H., Cocke, C., Gomes, J., Morkovsky, P., Parga, J., Peterson, E., & Garcia, C. (2007). Electrochemical generation of green rust with electrocoagulation. *ECS Trans.*, *3*(3), 67 – 76.

Mouedhen, G., Feki, M., De Petris Wery, M., & Ayedi, H. (2008). Behavior of aluminum electrodes in electrocoagulation process. *Journal of Hazardous Materials*, *150*, 124 – 135.

Noubactep, C. (2010). The fundamental mechanism of aqueous contaminant removal by metallic iron. *Water SA*, *4738*, 663–671.

Nouri, J., Mahvi, A., & Bazrafshan, E. (2010). Application of Electrocoagulation Process in Removal of Zinc and Copper From Aqueous Solutions by Aluminum Electrodes. *Int. J. Environ. Res.*, *4*(2), 201–208.

NSF/ANSI (2012). Drinking Water Treatment Units – Health Effects. NSF/ANSI 53 - 2011a.

Ozyonar, F., & Karagozoglu, B. (2014). Investigation of technical and economic analysis of electrocoagulation process for the treatment of great and small cattle slaughterhouse wastewater. *Desalination and Water Treatment*, *52*(1-3), 74–87.

Parga, J., González, G., Moreno, H., & Valenzuela, J. (2012). Thermodynamic studies of the strontium adsorption on iron species generated by electrocoagulation. *Desalination and Water Treatment*, *37*(1-3), 244–252.

Parga, J. R., Cocke, D. L., Valenzuela, J. L., Gomes, J. a., Kesmez, M., Irwin, G., Moreno, H., & Weir, M. (2005). Arsenic removal via electrocoagulation from heavy metal contaminated groundwater in La Comarca Lagunera México. *Journal of Hazardous Materials*, *124*(1-3), 247–54.

Perng, Y.-s., Wang, E. I.-c., Yu, S.-t., & Chang, A.-y. (2009). Application of a Pilot-Scale Pulsed Electrocoagulation system to OCC-Based Paper Mill Effluent. *TAPPI Journal*, *March 2009*.

Powell Water Systems, Inc. (2002). http://powellwater.com/product2.htm. Accessed: 4-09-2015.

Quantum Ionics, Inc. (2004). http://www.quantum-ionics.com/product2.shtml. Accessed: 11-30-2013.

Radić, S., Vujčić, V., Želimira Cvetković, Cvjetko, P., & Oreščanin, V. (2014). The efficiency of combined CaO/electrochemical treatment in removal of acid mine drainage induced toxicity and genotoxicity. *Science of The Total Environment*, *466–467*, 84 – 89.

Ratna Kumar, P., Chaudhari, S., Khilar, K. C., & Mahajan, S. P. (2004). Removal of arsenic from water by electrocoagulation. *Chemosphere*, *55*(9), 1245–52.

Sawyer, C., McCarty, P., & Parkin, G. (2003). *Chemistry for Environmental Engineering and Science*. Boston: McGraw Hill, 5 ed.

Smith, A. H., Lingas, E. O., & Rahman, M. (2000). Contamination of drinking-water by arsenic in Bangladesh : a public health emergency. *Bulletin of the World Health Organization*, *78*(9).

Snoeyink, V., & Jenkins, D. (1980). *Water Chemistry*. New York: John Wiley & Sons.

Tanneru, C., & Chellam, S. (2012). Mechanisms of virus control during iron electrocoagulation-microfiltration of surface water. *Water Research*, *46*, 2111 – 2120.

Tanneru, C., Rimer, J., & Chellam, S. (2013). Sweep flocculation and adsorption of viruses on aluminum flocs during electrochemical treatment prior to surface water microfiltration. *Environ. Sci. Technol.*, *47*, 4612 – 4618.

Terres-Martos, C., Navarro-Alarcon, M., Martin-Lagos, F., Gimenez-Martinez, R., Lopez-Garcia De La Serrana, H., & Lopez-Martinez, M. (2002). Determination of zinc levels in waters from southeastern Spain by electrothermal atomic absorption spectrometry : relationship with industrial activity. *Water Research*, *36*, 1912–1916.

US EPA (2009). National primary drinking water regulations. EPA 816-F-09-004.

van Genuchten, C., Pena, J., Amrose, S., & Gadgil, A. (2014). Structure of fe(iii) precipitates generated by the electrolytic dissolution of fe(0) in the presence of groundwater ions. *Geochimica et Cosmochimica Acta*, *127*, 285 – 304.

Vasudevan, S., & Lakshmi, J. (2011). Studies relating to an electrochemically assisted coagulation for the removal of chromium from water using zinc anode. *Water Science & Technology: Water Supply*, *11*(2), 142.

Vepsäläinen, M., Pulliainen, M., & Sillanpää, M. (2012). Effect of electrochemical cell structure on natural organic matter (NOM) removal from surface water through electrocoagulation (EC). *Separation and Purification Technology*, *99*(2012), 20–27.

Vik, E. A., Carlson, D. A., Eikum, A. S., & Gjessing, E. T. (1984). Electrocoagulation of potable water. *Water Research*, *18*(11), 1355–1360.

Wan, W., Pepping, T. J., Banerji, T., Chaudhari, S., & Giammar, D. E. (2011). Effects of water chemistry on arsenic removal from drinking water by electrocoagulation. *Water Research*, *45*(1), 384–92.

Water Tectonics (2015). http://www.watertectonics.com/technologies/. Accessed: 4-09-2015.

World Health Organization (1996). Copper in Drinking-water. WHO/SDE/WSH/03.04/88.

World Health Organization (2003a). Chromium in Drinking-water. WHO/SDE/WSH/03.04/04.

World Health Organization (2003b). Iron in drinking-water. WHO/SDE/WSH/03.04/08.

World Health Organization (2003c). Lead in drinking-water. WHO/SDE/WSH/03.04/09/Rev/1.

World Health Organization (2005). Nickel in Drinking-water. WHO/SDE/WSH/05.08/55.

Wright, M. R. (2007). *An Introduction to Aqueous Electrolyte Solutions*. West Sussex: John Wiley & Sons.

Zhu, B., Clifford, D., & Chellam, S. (2005). Comparison of electrocoagulation and chemical coagulation pretreatment for enhanced virus removal using microfiltration membranes. *Water Research*, *39*, 3098 – 3108.

A. APPENDICES

A.1. Chemical equilibrium models

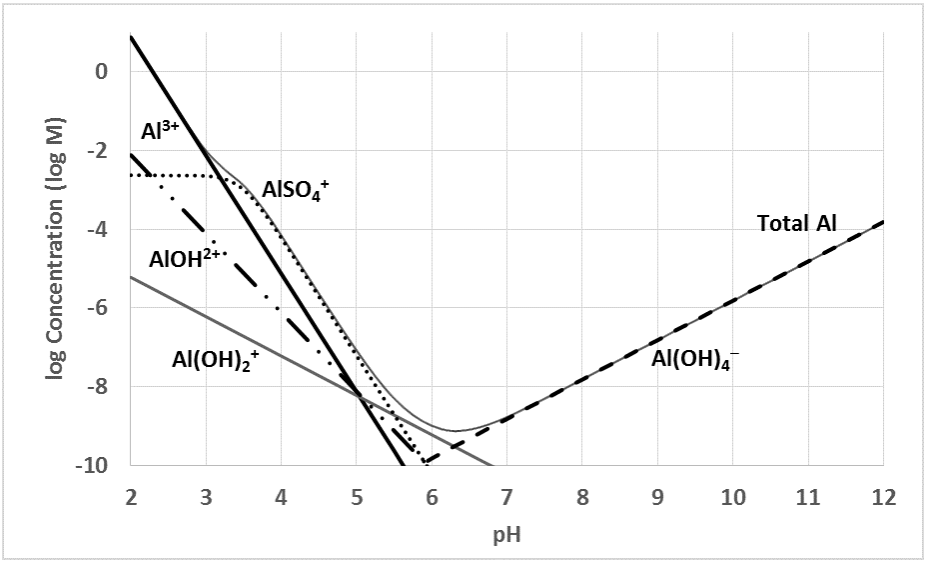

Figure A.1: Aluminum solubility and major soluble species, pH 2 to pH 12. Modeled with MINEQL+ software (see Section 2.3.)

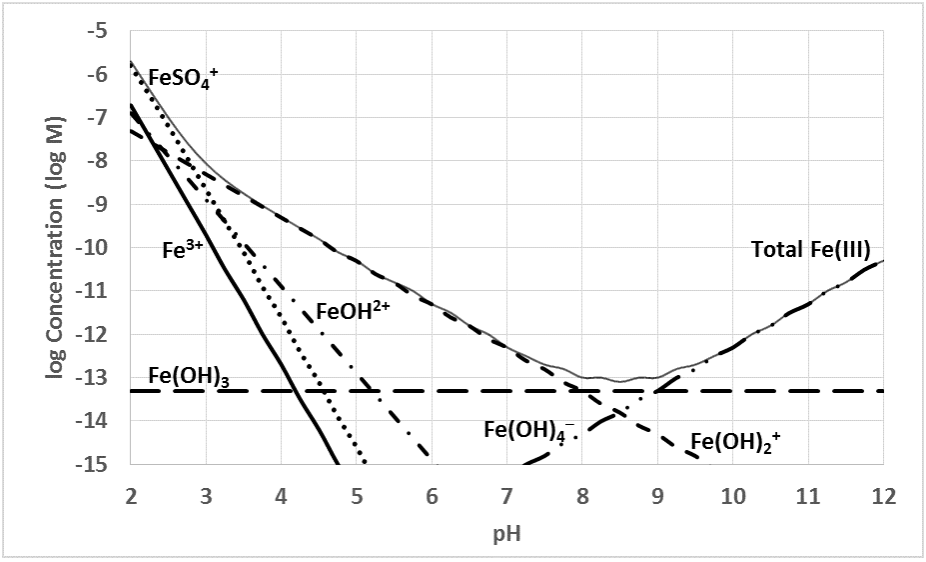

Figure A.2: Iron (III) solubility and major soluble species, pH 2 to pH 12. Modeled with MINEQL+ software (see Section 2.3.)

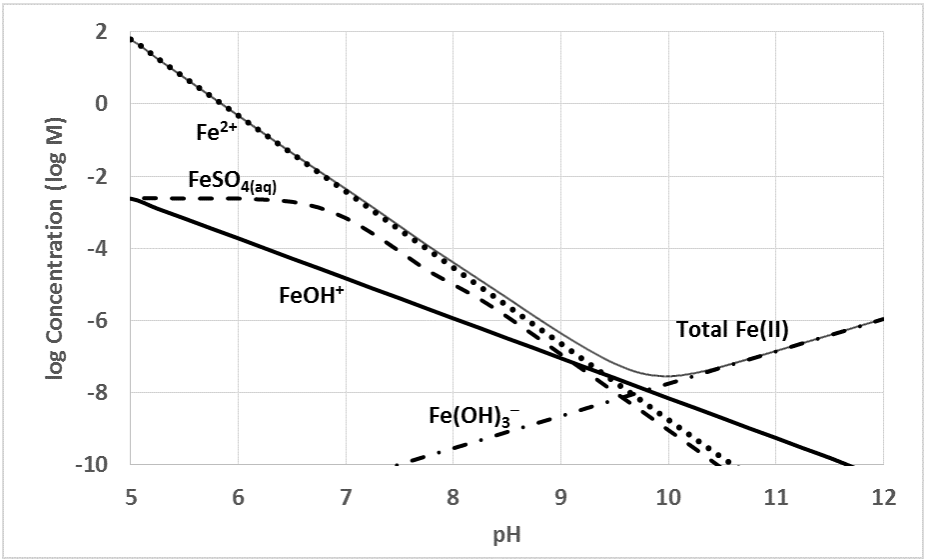

Figure A.3: Iron (II) and solubility and major soluble species, pH 5 to pH 12. Modeled with MINEQL+ software (see Section 2.3.)

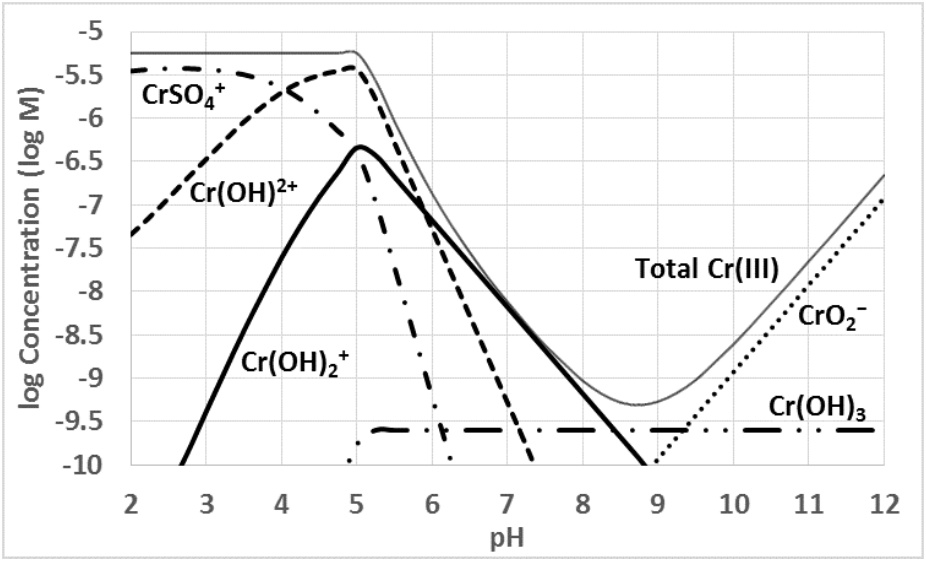

Figure A.4: Soluble species of chromium (III) with change in pH. Chromium speciation was modeled in a high-solids groundwater at a spiked concentration of $5.66x10^{-6}$ M Cr(III) using MINEQL+ software (see Section 2.3.)

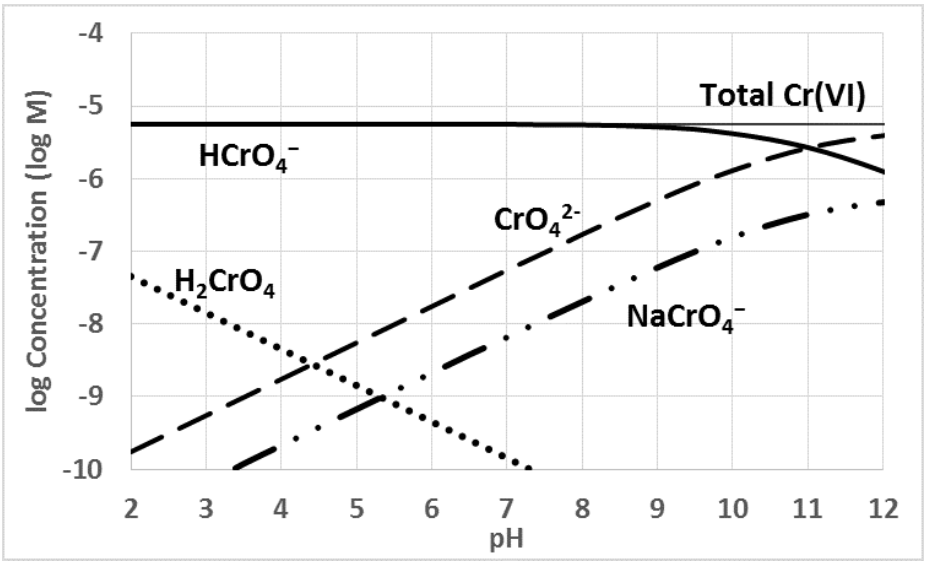

Figure A.5: Soluble species of chromium (VI) with change in pH. Chromium speciation was modeled in a high-solids groundwater at a spiked concentration of $5.66x10^{-6}$ M Cr(VI) using MINEQL+ software (see Section 2.3.)

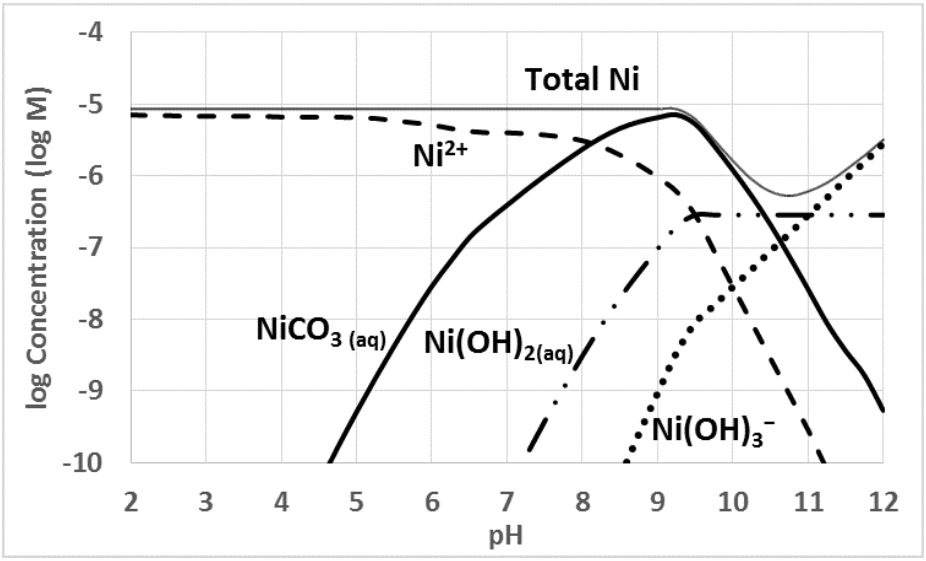

Figure A.6: Soluble species of nickel (II) with change in pH. Nickel speciation was modeled in a high-solids groundwater at a spiked concentration of $8.51x10^{-6}$ M Ni(II) using MINEQL+ software (see Section 2.3.)

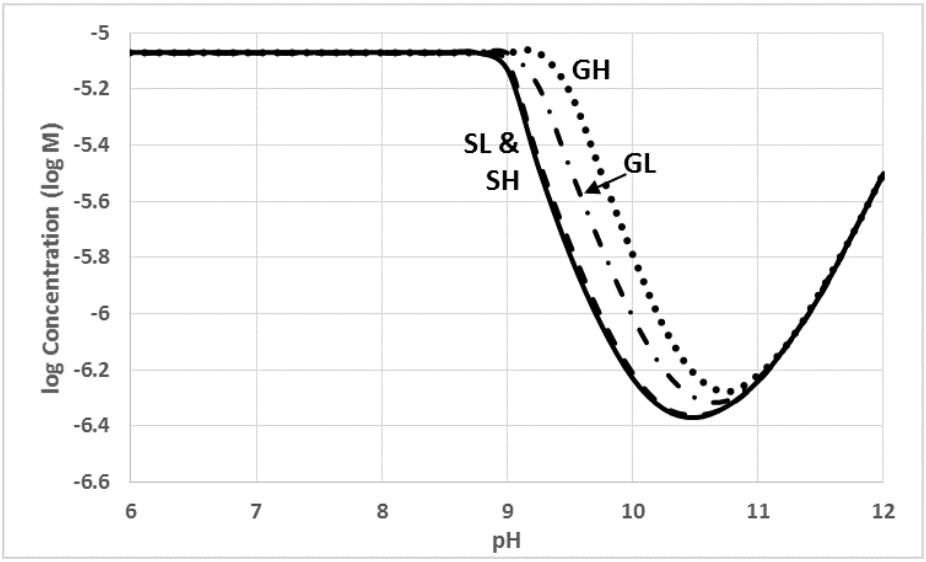

Figure A.7: Variation in nickel solubility with pH at a spiked concentration of $8.51x10^{-6}$ M Ni(II) in four synthetic test waters: "surface low" (SL), "surface high" (SH), "ground low" (GL), and "ground high." See Section 2.2 for a description of the test waters used in this study. Modeled with MINEQL+ software (see Section 2.3.)

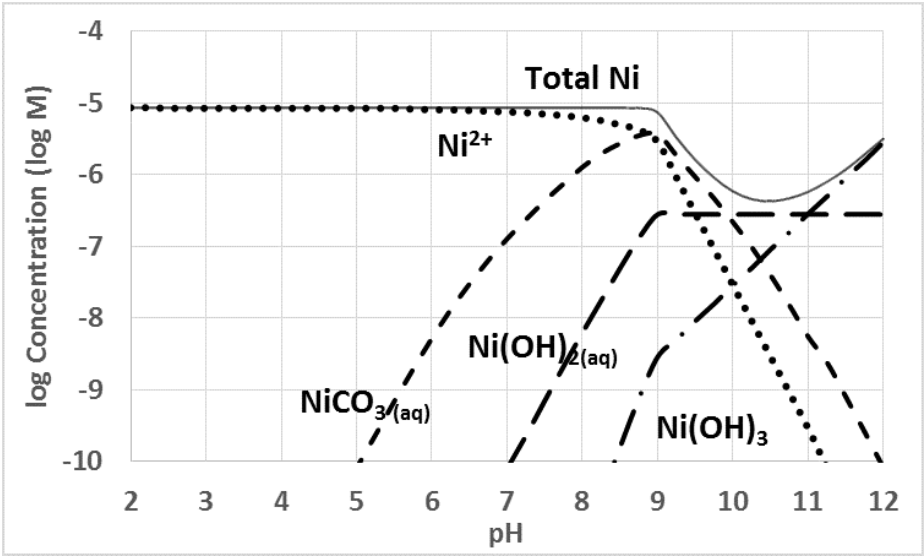

Figure A.8: Soluble species of nickel (II) with change in pH in low solids water. Nickel speciation was modeled in "surface low" test water at a spiked concentration of $8.51x10^{-6}$ M Ni(II) using MINEQL+ software (see Section 2.3.)

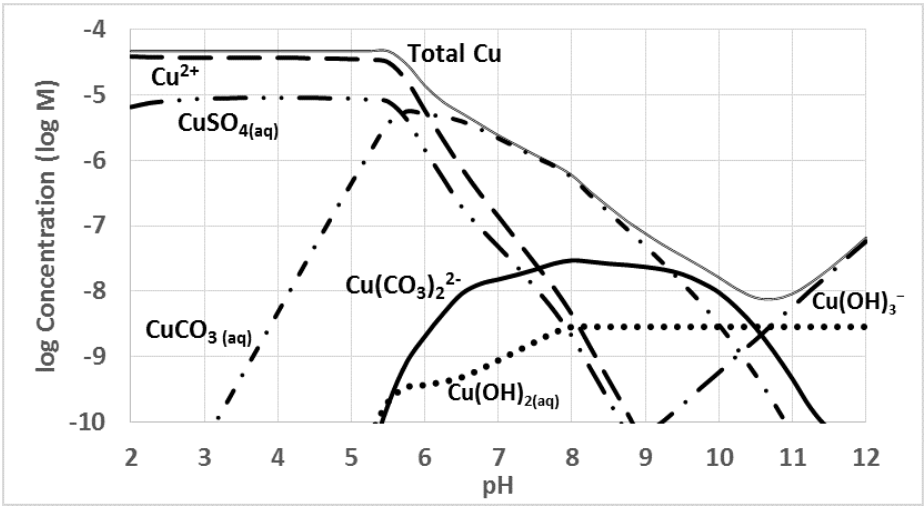

Figure A.9: Soluble species of copper (II) with change in pH. Copper speciation was modeled in a high-solids groundwater at a spiked concentration of $4.72x10^{-5}$ M Cu(II) using MINEQL+ software (see Section 2.3.)

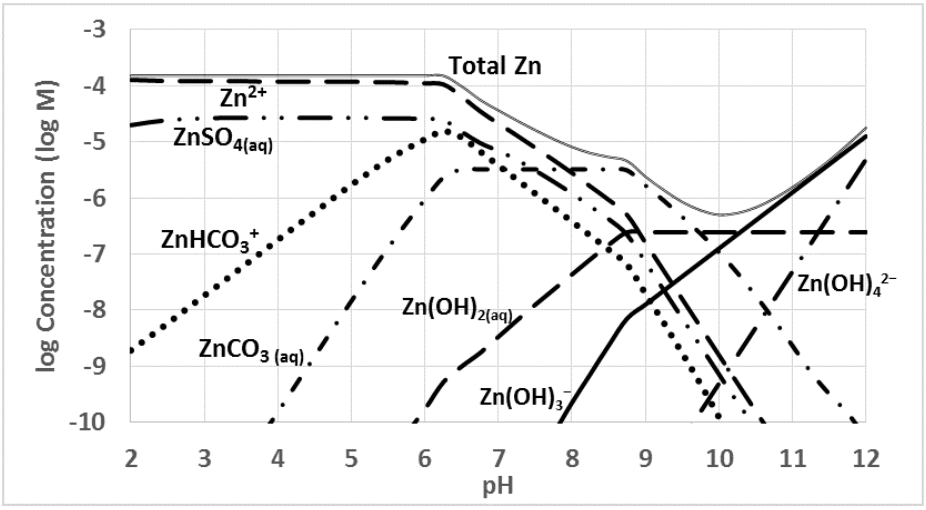

Figure A.10: Soluble species of zinc (II) with change in pH. Zinc speciation was modeled in a high-solids groundwater at a spiked concentration of $1.53x10^{-4}$ M Zn(II) using MINEQL+ software (see Section 2.3.)

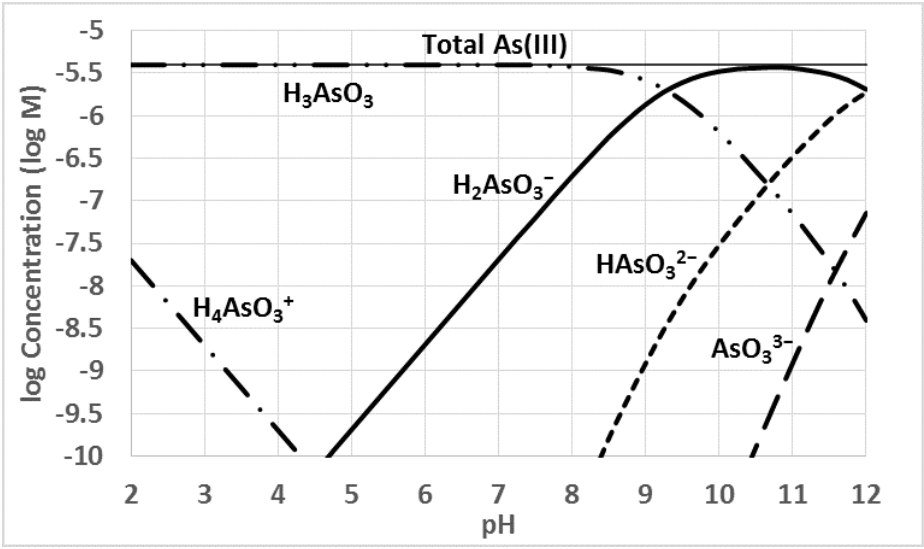

Figure A.11: Soluble species of arsenic (III) with change in pH. Arsenic speciation was modeled in a high-solids groundwater at a spiked concentration of $4.00x10^{-6}$ M As(III) using MINEQL+ software (see Section 2.3.)

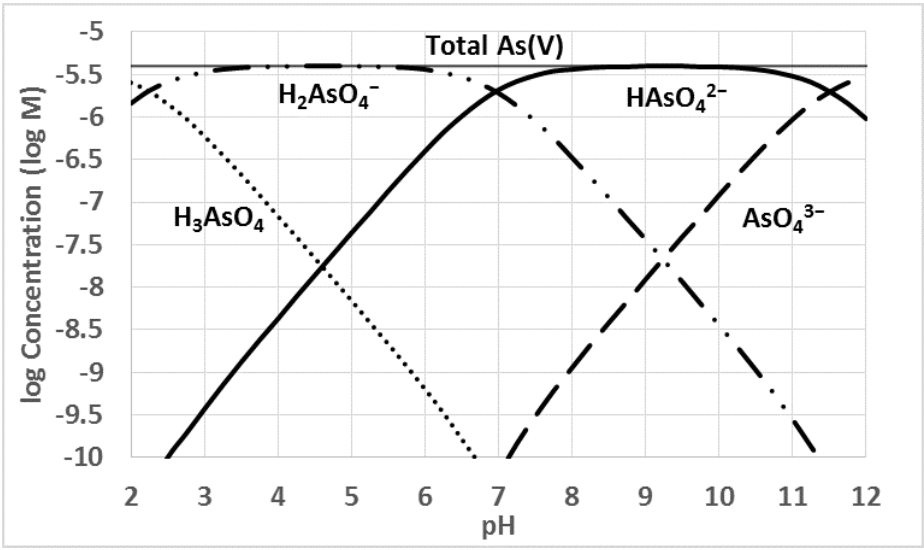

Figure A.12: Soluble species of arsenic (V) with change in pH. Arsenic speciation was modeled in a high-solids groundwater at a spiked concentration of $4.00x10^{-6}$ M As(V) using MINEQL+ software (see Section 2.3.)

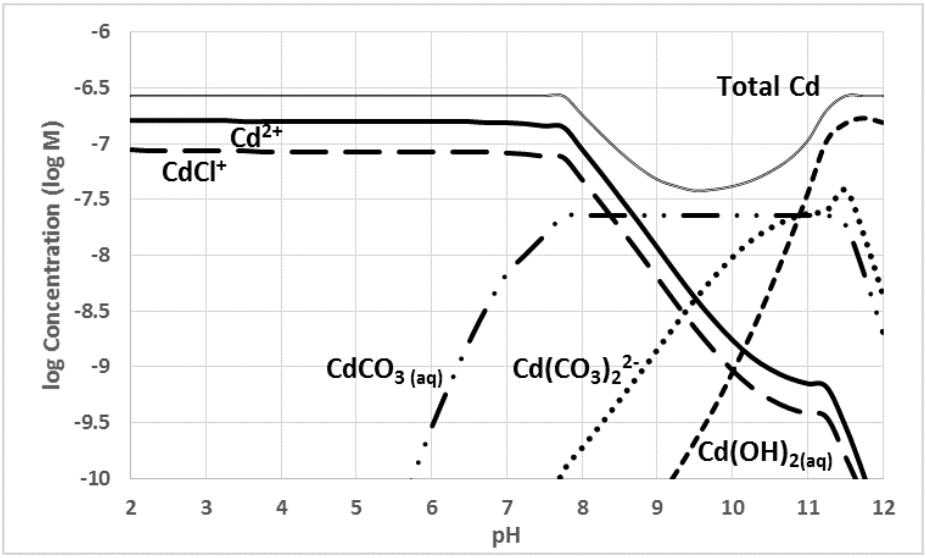

Figure A.13: Soluble species of cadmium (II) with change in pH. Cadmium speciation was modeled in a high-solids groundwater at a spiked concentration of $2.67x10^{-7}$ M Cd(II) using MINEQL+ software (see Section 2.3.)

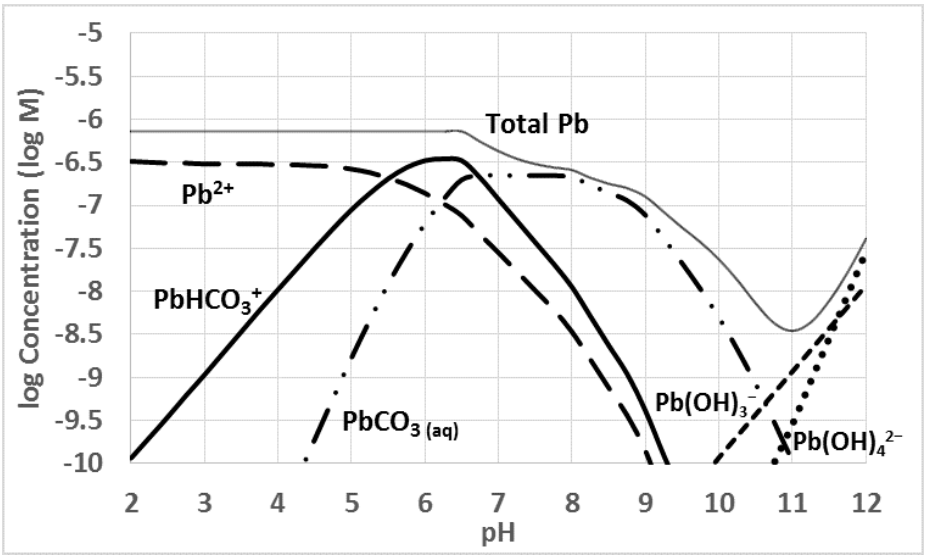

Figure A.14: Soluble species of lead (II) with change in pH. Lead speciation was modeled in a high-solids groundwater at a spiked concentration of $7.24x10^{-7}$ M Pb(II) using MINEQL+ software (see Section 2.3.)

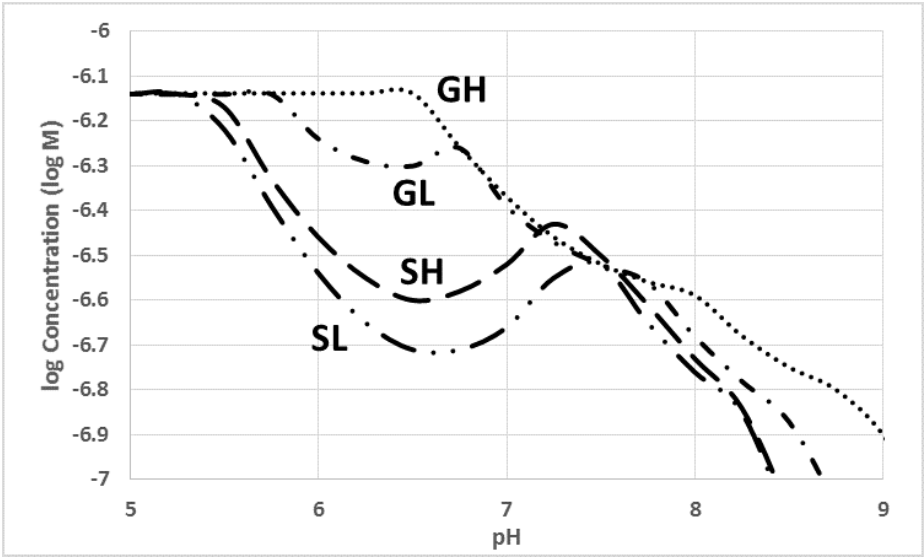

Figure A.15: Variation in lead solubility with pH in four synthetic test waters: "surface low" (SL), "surface high" (SH), "ground low" (GL), and "ground high". See Section 2.2 for a description of the test waters used in this study. Solubility at pH 6.5 is dependent on carbonate concentration (see also Figure A.14). Modeled with MINEQL+ software (see Section 2.3.)

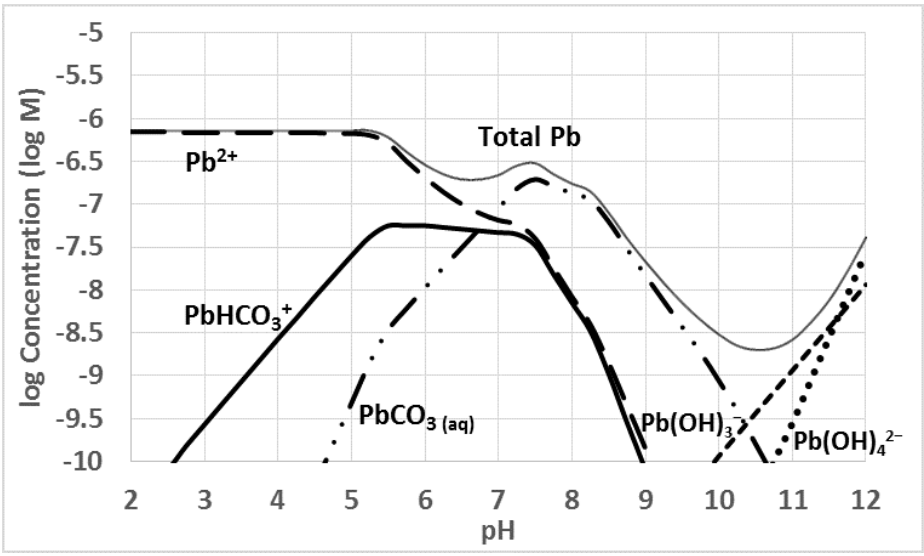

Figure A.16: Soluble species of lead (II) with change in pH in low solids water. Lead speciation was modeled in "surface low" test water at a spiked concentration of $7.24x10^{-7}$ M Pb(II) using MINEQL+ software (see Section 2.3.)

A.2. Test water formulations

Table A.1: Formulation of test waters using ACS-grade reagents. Concentrations are given in mg/L.

	Surface low	Surface high	Ground low	Ground high
Salts added				
$MgCl_2 \cdot 6\,H_2O$	36.8	67.8	284.4	362.2
$CaSO_4$	9.1	31.2	119.0	286.0
$CaCl_2 \cdot 2\,H_2O$	48.9	98.4	208.9	120.3
NaCl	0.0	0.0	0.0	800.9
$NaHCO_3$	100.8	163.8	466.7	763.3
Water quality				
Hardness (as $CaCO_3$)	58.0	123.2	369.3	470.0
TDS	164.0	301.0	876.7	2110.6